SLAC-PUB-2217
October 1978
(T/E)

CONF-780781--1

# HADRON AND PHOTON PRODUCTION AT LARGE TRANSVERSE MOMENTUM AND THE DYNAMICS OF QCD JETS*



S. J. Brodsky
Stanford Linear Accelerator Center
Stanford University, Stanford, California 94305

## ABSTRACT

The phenomenology of hadron and photon reactions at short distances is discussed in terms of perturbative quantum chromodynamics. In addition to large $p_T$ hadron reactions, we review predictions for jet production in two photon collisions, the relationship of photon and gluon jet production, hadronic production and color separation, upsilon decay into hadrons and photons, leading particle distributions in low $p_T$ hadron collisions, discriminants of quark and gluon jets, and the effects of coherence on gluon distributions in hadrons. A number of new experimental tests of QCD are discussed.

(Invited talk presented at the symposium on Jets in High Energy Collisions, Niels Bohr Institute and Nordita, July 10-14, 1978, to be published in Physica Scripta.)

* Work supported by the Department of Energy under contract no. EY-76-C-03-0515.



## 1. Introduction

The most direct tests of the interactions of quarks and gluons at short distances involve the production of single hadrons, hadronic jets, and photons at large transverse momentum. In this talk we will review several areas of hadronic phenomenology which test predictions of quantum chromodynamics calculated from perturbation theory, including:

(a) Jet production in two-photon reactions.[1] The cross sections for reactions such as $e^+e^- \to e^+e^- + \text{Jet} + X$ are readily calculated in perturbative QCD and turn out to be surprisingly large.

(b) The production of direct photons at large transverse momentum in hadron-hadron collisions.[2] In perturbative QCD, the ratio of gluon jet and direct photon cross sections is directly calculable, and leads to important phenomenological constraints.

(c) The multiplicity and distribution of hadrons in inclusive reactions may be related to color separation of the initiating subprocesses.[3,4] The consequences of this ansatz for gluon and quark jets are discussed. We also review other possible discriminants of jet parentage.

(d) The hadronic decay of the upsilon via three gluon jet[5,6] or a photon plus two gluon jets[6] could provide some of the most definite tests of QCD.

(e) Gluon jets may be "oblate" with principal axes correlated with the gluon polarization.[7]

(f) The gluon distribution of a hadron is connected with the size of the source due to coherent effects and is not determined solely by the quark distribution.[8]

At present, the most controversial area of QCD phenomenology concerns the production of single hadrons at large transverse momentum in proton-proton collisions.[9,10] We shall begin our discussion with a short review of the current issues.

## II. Production of Large Transverse Momentum Particles in Hadron-Hadron Collisions

There are currently two main approaches to large $p_T$ phenomena -- both based on perturbative QCD and a "hard scattering expansion."

(A) Quark, gluon scattering models. The basic collision subprocesses responsible for the large momentum transfer are assumed to be $qq \to qq$, $qg \to qg$, and $gg \to gg$, as calculated in Born approximation QCD.[11] Violation of scale-invariance occurs through the running coupling constant $\alpha_s(Q^2)$, the quark and gluon structure functions, and the transverse momentum ($k_T$) distributions of the constituents in the hadronic wave functions. The calculations automatically include those parts of higher particle number subprocesses such as $qq \to qqg$ which contribute to logarithmic scaling violations in the structure functions.

(B) The Constituent Interchange Model.[12] In addition to all of the contributions listed in (A), QCD also predicts "higher twist" subprocesses[13] where more than the minimal number of quark and gluon fields participate in the hard scattering reaction, such as $qM \to qM'$, $qB \to qB'$, $gq \to Mq$, $q\bar{q} \to M\bar{M}$, etc. Here "M" and "B" indicate $q\bar{q}$ and $qqq$ clusters of fixed mass relative to $p_T$. The cross sections for these subprocesses are readily computed from minimal QCD diagrams.[13,14] As in (A) logarithmic scaling violations occur.[15]

By definition, higher twist subprocesses are responsible for all large $p_T$ exclusive reactions involving hadrons.

The basic distinction between these two approaches for an inclusive reaction such as $pp \to \pi X$ is simply whether (a) the high $p_T$ trigger meson is formed after the hard scattering (e.g., $q_1 q_2 \to q_1 q_2$ with $q_1 \to q_1 + \pi$) or (b) formed before the collision and then scattered (e.g., $\pi q \to \pi q$). Obviously both types of subprocesses contribute to the cross section at some level -- it is a question of kinematics where each dominates: for fixed $x_T = 2p_T/\sqrt{s}$ and $\theta_{cm}$, the Born contributions clearly dominate at $p_T \to \infty$ since

$$\frac{\frac{d\sigma}{dt}(\pi q \to \pi q)}{\frac{d\sigma}{dt}(qq \to qq)} \sim F_\pi^2(p_T^2) \sim 0\left[\frac{1\ \text{GeV}^4}{p_T^4}\right] . \qquad \text{(II.1)}$$

On the other hand, the necessity for final state fragmentation in any quark or gluon scattering reaction implies a numerical suppression of the cross section by 2 to 3 orders of magnitude! This crucial factor (called "trigger bias" by Ellis, Jacob, and Landshoff[16]) results because a quark typically gives 75% of its momentum to the trigger particle due to its rapidly falling fragmentation function $G_{\pi/q}(z)$ at $z \sim 1$. The $qq \to qq$ subprocess then occurs at an effectively higher $p_T$ where the cross section is orders of magnitude smaller. (It is this effect that yields large jet/single ratios, since the (quark or gluon) jet trigger is not suppressed by this effect.) On the other hand, if the pion trigger emerges directly from the subprocess (as in the CIM $Mq \to \pi q$ subprocesses) then there is no trigger bias suppression. Thus for some range of $p_T$, the "higher twist" QCD-CIM subprocesses will be numerically important. Ignoring (logarithmic) scale-

violating effects the cross sections have the representative forms (see Fig. 1)

$$\text{QCD-Born:} \qquad \frac{d\sigma}{d^3p/E}(pp \to \pi X) \sim \frac{\alpha_s^2}{(100)p_T^4}(1 - x_T)^9 \qquad \text{(II.2)}$$

versus

$$\text{QCD-CIM:} \qquad \frac{d\sigma}{d^3p/E}(pp \to \pi X) \sim \frac{\alpha_M^2}{p_T^8}(1 - x_T)^9 \qquad \text{(II.3)}$$

The critical question is determining the magnitude of each contribution.

In principle, it is straightforward to determine the normalization of the $2 \to 2$ QCD subprocesses contributing to the inclusive cross section, since $\alpha_s$ and the structure functions are to a large extent determined (although there is some uncertainty in determining the gluon distributions in hadrons). The effect of the $k_T$ distributions of the hadronic constituents is controversial. An essential point ignored in many model calculation is that the interacting constituents are always off the mass shell and spacelike:[17]

$$k^2 = -\frac{\vec{k}_T^2 + \tilde{m}^2}{1 - x} \qquad \text{(II.4)}$$

where $\tilde{m}^2$ is a linear combination of squares of spectator and incident hadron masses. The off-shell kinematics ensure that the gluon pole in the $qq \to qq$ amplitude never occurs in the physical region, and serves to damp out the effects of large $k_T$. In practice, one finds that $k_T$ fluctuations do not increase the inclusive cross section by more than a factor of 2 for $p_T \geq 2$ GeV, even if we assume very large mean $k_T \sim 850$ MeV Gaussian smearing.[18] A representative calculation is shown in Fig. 2. (If one uses on-shell kinematics, the cross section can be increased by an arbitrary amount depending on a cut-off.) Off-shell kinematics are of course required whether

one uses covariant Feynman amplitudes or time-ordered perturbation theory.

The cross section for subprocesses such as $qM \to qM$ has the form[19]

$$\frac{d\sigma}{dt}(qM \to qM) = \frac{\pi\alpha_M^2}{su^3} \qquad \text{(II.5)}$$

corresponding to the QCD amplitude shown in Fig. 1(d). The $qM \to qM$ amplitude falls as $s^{-1}$ at fixed u because of the exchanged fermion in the u-channel. The power fall-off at fixed center-of-mass angle agrees with the dimensional counting rules $d\sigma/dt \propto s^{-(n-2)}$ where n (= 6 here) is the number of active fields in the initial and final state.[20] The constant $\alpha_M$ is proportional to $\alpha_s(p_T^2)$ times the meson wavefunction at the origin. It can be fixed phenomenologically (to within a factor of $\sim$2), since the $qM \to qM$ amplitude enters directly in the meson elastic form factor and meson-proton elastic scattering at large momentum transfer (see Fig. 3). In a recent paper, Blankenbecler, Gunion and I have found that within errors of order $\pm$50%, $\alpha_M \gtrsim 2$ GeV$^2$.[19]

In order to determine the size of the contribution of the $Mq \to Mq$ subprocess to the $pp \to \pi X$ (see Fig. 4) we also need the normalization of $G_{M/p}(x)$, the distribution of virtual $q\bar{q}$ states in the proton. (The same normalization enters virtual meson-induced reactions, such as Deck or Drell diagrams in low t hadronic physics and the height of the meson plateau in forward reactions.) We have assumed a normalization such that $\sim$1/2 of the $\bar{q}$ sea can be identified as constituents of the virtual $q\bar{q}$ states.

With these normalizations, we find that contributions (B) are in fact consistent with the normalization of FNAL[21] and ISR data[22] for $pp \to \pi X$ up to $p_T \sim 8$ to 10 GeV. At that point we predict the $2 \to 2$ QCD - Born sub-processes contributions (A) will cross over and dominate the inclusive cross

section.[19,22] (See Fig. 5.) Moreover, we note the following:

(1) The best power-law fit to the Chicago-Princeton[21] FNAL data is

$$E\frac{d\sigma}{d^3p}(pp \to \pi^+X) = \frac{1}{p_T^{8.2\pm.5}}(1-x_T)^{9.0\pm0.5} \qquad (II.6)$$

is agreement with the predicted CIM powers.

(2) The best fit[24] to the angular distribution of the subprocess in $pp \to \pi X$ is $d\sigma/dt \propto 1/su^3$ or $1/st^3$ in agreement with the predicted CIM form.

(3) The CIM mechanism predicts that the trigger particle usually emerges <u>alone</u> without same-side correlated particles, or from the decay of resonances, especially the $\rho$. This is in excellent agreement with the results of the British-French-Scandinavian[25] group's experiment at the ISR, who find that in ~85% of the events with a 4 GeV trigger, the trigger particle is unaccompanied by same-side charged particles (aside from the usual low momentum background). The small growth of the same-side momentum with the trigger $p_T$ observed in the experiment indicates that on average more than 90% of the trigger momentum is carried by the trigger pion -- much larger than the ~75% expected from q or g jet fragmentation.[26] The BSF data clearly does not support the hypothesis that the same-side jet is a quark or gluon jet.

(4) The $qM \to qM$ subprocesses implies that flavor is generally exchanged in the hard scattering reaction.[27] For example, consider the quark interchange and $q\bar{q} \to M\bar{M}$ fusion contributions to $pp \to K^{\pm}X$ shown in Fig. 6. The average charge of the recoil quark is slightly positive for the $K^+$ trigger and > +1/3 for the case of the $K^-$ trigger. Thus the charge and flavor of the away-side jet in the CIM can be correlated with the flavor quantum numbers of the trigger. In contrast, gluon exchange diagrams

predict very small[26] flavor correlations between the away-side and same-side systems. The data from the BSF-ISR group (see Fig. 7) for various charge triggers at 90° show striking flavor correlations, especially for $K^-$ and $\bar{p}$ triggers, in general agreement with the above expectations for the quark exchange processes of the CIM model. (A possible difficulty, however, may be the absence of a strong difference in the away side +/- ratio for $\pi^+$ and $\pi^-$ triggers. This may be due to the fact that resonance decays, particularily $\rho^0 \to \pi^+\pi^-$, dilute the charge correlations.) It should be emphasized that the CIM terms are not maximal for back to back configurations because of the difference in q and M distributions. [This could explain why charge correlations are strongest away from zero rapidity on the away side in the BSF-ISR[25] experiment and why only minimal flavor correlations are observed in the FNAL experiment of R. J. Fisk et al.,[28] who only look at particles directly opposite a 90° trigger. The correlations will also be reduced because of the nuclear target.]

In each case we would expect that these charge correlations will disappear at very high $p_T$ when the 2 → 2 QCD - Born subprocesses become dominant. It is interesting to note that for $K^-$ and $\bar{p}$ triggers, the cross-over point is predicted by Jones and Gunion[23] to occur (for pp collisions) at a relatively small $p_T$ (~4 to 5 GeV at ISR energies) due to the rapid fall-off of the CIM terms as $x_T \to 1$ for these triggers. Thus there is a rich, dynamical structure controlled by the $p_T$ and $x_T$ kinematics which can be unraveled by quantum number correlations.

(5) In the case of pp → pX, the dominant CIM subprocess is the qB → qp subprocess. The theoretical prediction is $E\, d\sigma/d^3p\ (pp \to pX) \approx p_T^{-12}(1 - x_T)^7$. The Chicago-Princeton[21] fit at 90° in fact gives $p_T^{-11.7}(1-x_T)^{6.8}$

at FNAL energies, $p_T < 7$ GeV with uncertainties in the exponent of order ±0.5. We emphasize that a successful model for single particle production must account for both high $p_T$ meson and baryon data. There does not seem any way to account for the $pp \to pX$ scaling behavior in terms of $2 \to 2$ QCD subprocesses without enormous scale-breaking in the $q \to p$ distribution function; we note that data from DESY for $e^+e^- \to \bar{p}X$ appears to be reasonably consistent with scale-invariance. On the other hand, we find that the normalization of the $Bq \to Bq$ subprocess required here is consistent with elastic $pp \to pp$ scattering and the proton form factor.[19] In addition, at $\theta_{cm} = 90^\circ$, $x_T > 0.6$, we predict that the direct scattering process $pq \to pq$ (where the incident proton itself scatters in the subprocess) should become dominant, leading to $p_T^{-12}(1-x_T)^3$ behavior. The direct scattering contribution to inclusive $pp \to pX$ connects smoothly to elastic scattering $pp \to pp$, in agreement with the Bjorken-Kogut "correspondence principle" arguments.[29]

Combining the QCD 2-2 Born subprocess contributions with the CIM (higher twist QCD) contributions leads to a combined prediction for $pp \to \pi^+X^-$ of the form ($\theta_{cm} = 90^\circ$)[19]

$$E\frac{d\sigma}{d^3p}(pp \to \pi^+X^-) = \alpha_s(p_T^2)\ (0.035)\ \frac{(1-x_T)^9}{p_T^4} + (9)\ \frac{(1-x_T)^9}{p_T^8}\ , \tag{II.7}$$

in GeV units. The 0.035 factor includes the suppression factor due to trigger bias[16] from $q \to M+q$ fragmentation as discussed above. (The factor of 9 in the CIM term is computed using $\alpha_H = 2$ GeV$^2$ and an estimated factor of 2 from resonance decay contributions to inclusive $\pi^+$ production.) The $(1-x_T)^9$ power comes from convolutions of valence distributions $G_{q/p}(x)$ with $(1-x)^3$ fall-off and $G_{\pi/q} \sim (1-x)^5$. Asymptotic freedom,[5] spin correlations,

etc. can increase the effective power to $(1-x_T)^{10 \text{ or } 11}$. Thus at $p_T \sim$ 10 GeV, the 2 → 2 subprocesses are predicted to be dominant, the power of $p_T$ for $\pi^{\pm,o}$, $K^+$, and production should decrease to $p_T^{-6}$ and then asymptotically approach $p_T^{-4}$ scaling, modulo QCD logarithmic radiative corrections. At these values of $p_T$ all the canonical QCD predictions characteristic of the Born diagrams should hold; in particular the same-side system will cease to be dominated by single particles, and flavor correlations between the trigger and away-side system will tend to zero. An important prediction of QCD is the eventual dominance of gluon jet recoil.[11,26]

We note that recent ISR data[22] for the $pp \to \pi^o X$ cross section for $6 < p_T < 12$ GeV are indeed consistent with a sum of terms of the form of Eq. (II.7) (see Fig. 8). For $p_T < 8$ GeV, the experimental data are consistent with dominance of the CIM terms. We emphasize that the predicted QCD 2 → 2 Born contributions alone are at least a factor of 5 below the data for $p_T \sim 4$ GeV, even allowing for a factor of 2 from $k_T$ smearing corrections and uncertainties in the effective value of $\alpha_s$; in any event these contributions are inconsistent with all of the features of the data, (1) through (5) discussed above.

An important theoretical question is how to systematically include the effects of higher particle number hard-scattering subprocesses 2 → n and even n → n. In a recent paper by Caswell, Horgan, and myself[18] we showed that for $\phi^3$ field theory, the inclusive cross section for A+B → C+X can be computed systematically in terms of a sum of incoherent hard scattering contributions, as expected by parton-model considerations. In the $\phi^3$ model all effects associated with large $k_T$ in the incident wavefunction

are automatically included when the higher order subprocesses are taken into account. Subprocesses with higher number of active fields suffering the large momentum transfer give higher powers of $p_T$ fall-off.

The situation in QCD is best illustrated by an example (see Fig. 9). A Feynman diagram which corresponds to $qq \to qq$ scattering with gluon bremsstrahlung yields contributions to both the $qq \to qq$ hard scattering subprocess (when the emitted gluon $g_1$ is parallel to $q_1$) and to the $qg \to qg$ subprocess (when the exchanged gluon $g_2$ is at low $k_T$ relative to $q_2$). The contribution where the $q_3$, $q_4$, and g all emerge at different $\theta_{cm}$ is suppressed by a power of $\log p_T^2$. Note that (1) off-shell kinematics are required in order to obtain the correct contribution to the $gq \to gq$ subprocess; (2) it would be double-counting to include both $k_T$ fluctuations to $qq \to qq$ scattering plus the $gq \to gq$ subprocess; and (3) the leading logarithmic corrections to the $qq \to qq$ scattering are already included when the measured $G_{q/p}$ structure function is used. A consistent treatment in QCD requires simultaneous consideration of the hadronic wavefunctions, off-shell effects, and the $k_T$ fluctuations implicit in higher particle number subprocesses.

The theoretical origin of the $k_T$ distribution of the quark and gluon distributions in hadrons is complicated, since there are clearly several mechanisms at work:

(a) The tail of the hadronic wavefunction at large $k_T$ due to constituent recoil gives a contribution of order

$$\frac{dN}{dk_T^2} \sim \frac{a_M}{k_T^4} \qquad (m^2 \ll k_T^2 \ll p_T^2) \qquad \text{(II.8)}$$

(b) Radiative corrections due to single gluon recoil gives

$$\frac{dN}{dk_T^2} \sim \frac{\alpha_s(k_T^2)}{k_T^2} \qquad (m^2 \ll k_T \ll p_T^2) \qquad \text{(II.9)}$$

and eventually will dominant over (a). This contribution can also be identified with 2 → 3 QCD subprocesses.

(c) In any inclusive process in which color is virtually separated the radiated soft gluons taken together give an effective $k_T$ distribution. According to the analysis of Dokshitser, D'Yakanov, and Troyan[30] for the Drell-Yan process, the effective distribution has a computable Gaussian-like shape.

(d) The intrinsic $k_T$ distribution of the hadronic wavefunction due to binding and other non-perturbative effects. The recent bubble chamber measurements of the final state hadron distribution in deep inelastic neutrino-proton scattering reported at this meeting by Vander Velde[31] shows that the intrinsic $k_T$ of the constituents are in fact small; the fast hadrons near $x_F \gtrsim -1$ in the $W^+$-proton cm frame (from the spectator "qq" jet) have $\langle k_T^2 \rangle \gtrsim 0.1$ GeV$^2$. The large values of $k_T$ observed in Drell-Yan and large $p_T$ reactions (from $p_{out}$ distributions) thus must be attributed to a combination of the mechanics (a),(b), and (c).

As we discussed, the CIM (higher twist QCD) diagrams can temporarily dominate the 2 → 2 Born subprocess contributions because of the trigger bias in single particle high $p_T$ reactions. In the case of jet triggers, the trigger bias is absent, and the QCD Born terms are expected to be dominant even at $p_T \sim 4$ GeV. Thus jet experiments can provide a direct tool to check the basic form of QCD dynamics, verify the form and magnitude of the tri- and quartic-gluon interactions, etc. At present, there is a

great deal of uncertainty how to define a jet trigger, particularly because of possibly striking differences in the structure of gluon and quark jets. The study of jet production in two photon physics (see Section III) and the recoil system in deep inelastic scattering should be helpful for establishing workable definitions for jet triggers.

The CIM-QCD approach to large $p_T$ dynamics, combined with dimensional counting rules for determining the leading power behavior, makes a large number of phenomenological predictions (see Refs. 19,23). Thus far, I am not aware of any serious conflicts with data. In particular, the observed particle ratios such as $pp \to K^- X/pp \to K^+ X$ and beam ratios $\pi p \to \pi X/pp \to \pi X$ are not inconsistent with the CIM (although in the latter case, the situation is complicated by the presence of several competing subprocesses).

The dimensional counting rules,[14,20]

$$\frac{d\sigma}{dt}(A+B \to C+D) = \frac{F(\theta_{cm})}{(p_T^2)^{N_A+N_B+N_C+N_D-2}} \qquad \text{(II.10)}$$

for exclusive processes can be used to determine the overall $p_T$ power-law fall-off of each subprocess $a+b \to c+d$ in inclusive reactions. The rule emerges from computations of the minimally connected Born diagrams in QCD. Perturbative QCD corrections modify the result via finite powers of $\log p_T^2$.[32] Lepage, Brodsky, and Huang[32] have shown that when A,B,C, and D are hadrons, the Landshoff "pinch" singularities due to successive near-on-shell quark-quark scatterings are in fact asymptotically suppressed in QCD relative to the diagrams which give the dimensional counting rules. The crucial point is the presence of (Sudakov) form factors which suppress on-shell elastic $qq \to qq$ amplitudes (this is in agreement with an earlier ansatz of Polkinghorne[33] and Cornwall and Tiktopoulos[34]). (There are no eikonal-like

suppression factors for the minimally connected dimensional counting diagrams since the scattering constituents are far-off shell). The result (II.10) also predicts $F_A(t) \sim t^{1-n_A}$ (modulo a finite power of log t) for the asymptotic elastic (spin-averaged) electromagnetic form factor.

## III. Jets in Photon-Photon Collisions

One of the most direct tests of quantum chromodynamics at short distances is the study of particle production at large transverse momentum in photon-photon collisions. It is well known that the two photon process becomes an increasingly important source of hadrons in $e^+e^-$ collisions as the center of mass energy rises. The dominant part of the cross section for $e^+e^- \to e^+ + e^- +$ hadrons (Fig. 10(a)) arises from the annihilation of two nearly on-shell photons emitted at small angles to the beam. Photon-photon collisions allow the entire range of hadronic physics, as studied for example at the ISR for pp collisions, to be studied in $e^+e^-$ rings.[35] The crucial question, of course, is the rate. Recently, T. DeGrand, J. Gunion, J. Weis,[1] and I have shown that jet production at rather large $p_T$ for PEP and PETRA energies is predicted in perturbative QCD to occur at a remarkably large rate. For example, the cross section for the production of jets with total hadronic transverse momentum ($p_T > p_{T\min}$) from $\gamma\gamma \to q\bar{q}$ subprocess alone (Fig. 10(b)) is[1,36]

$$\sigma_{e^+e^- \to e^+e^- \text{ Jet}+X}(s, p_T^{\text{jet}} > p_T^{\min}) \simeq R_{\gamma\gamma}\, \sigma_{e^+e^- \to e^+e^- \mu^+\mu^-}(s, p_T^{\mu_\pm} > p_T^{\min})$$

$$\gtrsim R_{\gamma\gamma}\,\frac{32\pi\alpha^2}{3}\left(\frac{s}{2\pi}\log\frac{s}{m_e^2}\right)^2\frac{\left(\log\frac{s}{p_{T\min}^2}-\frac{19}{6}\right)}{p_{T\min}^2}$$

$$\gtrsim \frac{0.5\ \text{nb GeV}^2}{p_{T\min}^2}\quad\text{at}\quad\sqrt{s}=30\ \text{GeV}\ . \qquad \text{(III.1)}$$

where, in QCD perturbation theory, $R_{\gamma\gamma}=3\sum_q e_q^2=34/27$, above the charm threshold. For $p_{T\min}=4$ GeV, $\sqrt{s}=30$ GeV, this is equivalent to 0.3 of unit of R; i.e., 0.3 times the $e^+e^-\to\mu^+\mu^-$ rate. We note that at $\sqrt{s}=200$ GeV, the cross section from the $e^+e^-\to e^+e^-q\bar{q}$ subprocess with $p_{T\min}>10$ GeV is 0.02 ub, i.e.: about 9 units of R! At such energies $e^+e^-$ colliding beam machines are more nearly laboratories for $\gamma\gamma$ scattering than they are for $e^+e^-$ annihilation.

Photon-photon collisions at large $p_T$ provide an ideal laboratory for testing perturbative QCD. The $\gamma\gamma\to q\bar{q}$ reaction tests the scale-invariance of the quark propagator at large momentum transfer; higher order QCD corrections to $R_{\gamma\gamma}$ are of order $\alpha_c(p_T^2)/\pi$ and should be readily calculable, in analogy to the QCD corrections to the $e^+e^-\to q\bar{q}$ rate. The $\gamma\gamma\to q\bar{q}$ subprocess implies the production of two non-colinear, roughly coplanar high $p_T$ (SPEAR-like) jets, with a cross section nearly flat in rapidity. Such "short jets" will be readily distinguishable from $e^+e^-\to q\bar{q}$ events due to missing visible energy, even without tagging the forward leptons. If one measures the ratio to the $ee\to\mu^+\mu^-ee$ rate, ($R_{\gamma\gamma}$), the uncertainties due to tagging efficiency, the equivalent photon approximation, etc., cancel out.

In addition to 2-jet processes, QCD also predicts contributions to 3 and 4 jet final states from subprocesses such as $\gamma q\to gq$ (3-jet production) (Fig. 10(c)) where one photon interacts with the quark constituent of the other photon, and $qq\to qq$ (4 jet production) (Fig. 10(d)). Unlike hadron-

induced reactions, where ambiguities due to the structure functions are encountered, the structure function of the photon $G_{q/\gamma}(x,Q^2)$ has a perturbative component which can be predicted from first principles in QCD. This component, as first computed by Witten,[37] has the asymptotic form at large probe momentum $Q^2$

$$G_{q/\gamma}(x,Q^2) \Longrightarrow \frac{\alpha}{\alpha_s(Q^2)} f(x) + O(\alpha^2) \qquad \text{(III.2)}$$

i.e.; aside from an overall logarithmic factor, the $\gamma \to q$ distribution Bjorken scales; $f(x)$ is a known, calculable function. Unlike the proton structure function which contracts to $x = 0$ at infinite probe momentum $Q^2 \to \infty$, this component of the photon structure function increases as $\log Q^2$ independent of $x$. This striking fact is of course due to the direct $\gamma \to q\bar{q}$ perturbative component in the photon wavefunction. In addition one also expects a nominal hadronic component due to intermediate vector meson states.

A remarkable fact is that the $\alpha_s(p_T^2)$ factor in the denominator of the structure function of the photon cancels the $\alpha_s(p_T^2)$ factors in the $\gamma q \to gq$ or $qq \to qq$ at large $p_T^2$ subprocesses for both the 3-jet and 4-jet reactions. Thus the asymptotic cross section for $\gamma\gamma \to$ Jet + X at fixed $\theta_{cm}$ and $p_T/\sqrt{s}$ actually obeys perfect scale-invariance when all QCD perturbative corrections are taken into account![38]

Predictions from Ref. 1 for the jet cross section $\theta_{cm} = 90^0$ and $\sqrt{s} =$ 30 GeV are shown in Fig. 11. The $\gamma\gamma \to q\bar{q}$ subprocess is dominant above $p_T^{jet} = 4$ GeV. The jet topology allows an experimental separation of the 2,3 jet and 4, jet events. We have also shown in Reference 1 the cross section expected if strict vector-meson dominance were to hold, and photon-photon collisions were similar to meson-meson collisions. The direct perturbative point-like coupling of nearly-on-shell photons to the

quark current is the crucial new feature which allows such large high $p_T$ jet reactions. We also note that possible non-perturbative (absorption, instanton, etc.) effects which conceivably could effect the normalization of hadron-hadron reactions in close collisions should be absent for perturbative $\gamma\gamma$ reactions.

In the case of production of single particles at large $p_T$ in $\gamma\gamma$ collisions, the effect of trigger bias is again critical, and we expect $\gamma q \to Mq$ processes to strongly dominate q or g fragmentation reactions until very large $p_T$. A complete discussion is given in Ref. 2.

Thus the study of $\gamma\gamma$ collisions at large $p_T$ provides a detailed laboratory for the study of QCD dynamics of hadrons and photons at short distances. It will also be interesting to study the charm threshold in the $\gamma\gamma \to q\bar{q}$ reaction as well as the interplay of vector-meson-dominance and perturbative QCD dynamics as the momentum transfer increases. The photon mass and spin dependance of $\gamma$ induced reactions can be studied by tagging the scattered $e^{\pm}$ at large angles.

## IV. Photon Production at Large $P_t$

In addition to $\gamma\gamma$ collisions, other photon-induced reactions such as $\gamma p \to \pi X$, $\gamma p \to \gamma X$, and $\gamma p \to$ jet X are sensitive to "direct" QCD reactions such as $\gamma q \to Mq$, and $\gamma q \to \gamma q$, where the incident photon participates in the hard scattering subprocess (and no forward hadrons are produced)[39] as well as standard QCD or CIM subprocesses such as $qq \to qq$, $qM \to qM$, and $qM \to \gamma M$, where the perturbation QCD "anti-scaling" structure function of the incident photon is important.

Photon production at large $p_T$ can also be used as an important probe of the underlying hard scattering subprocesses.[2,40] Discarding photons which are produced from hadron decay ($\pi^o \to \gamma\gamma$, $\eta^o \to \gamma\gamma$, etc.), we can distinguish several mechanisms in QCD:

(a) QCD Born contributions with quark fragmentation, e.g.: $qq \to qq$, $gq \to gq$ with $q \to \gamma q$. The $G_{\gamma/q}(x,Q^2)$ fragmentation distribution has the Witten[37] anti-scaling form and is nearly flat in x until x very close to 1. If a QCD 2-2 subprocess dominates both $\pi$ and $\gamma$ production, then

$$\frac{\frac{d\sigma}{d^3p/E}(pp \to \gamma X)}{\frac{d\sigma}{d^3p/E}(pp \to \pi X)} \sim \frac{G_{\gamma/q}(x_T)}{G_{\pi/q}(x_T)} \sim \frac{a}{1-x_T} \qquad \text{(IV.1)}$$

at $\theta_{cm} = 90^o$, independent of $p_T$.

(b) Direct QCD Born contributions, from subprocesses such as:

$$gq \to \gamma q \qquad \text{and} \qquad q\bar{q} \to \gamma g \ .$$

In these processes the photon is produced in the subprocess itself. Since there are no accompanying trigger jet hadrons one can easily distinguish such reactions from fragmentation processes.[2] These reactions can also be important for producing massive lepton pairs at large transverse momentum.

(c) CIM-type subprocesses, such as $Mq \to \gamma q$, where the incident meson M is a correlated $q\bar{q}$ pair in the incident hadron wavefunction. Both processes (b) and (c) can dominate over (a) for moderate $p_T$ because of the absence of trigger bias suppression. The nominal scaling laws are[2]

$$E\frac{d\sigma}{d^3p}(pp \to \gamma X) \sim \begin{cases} \alpha_s^2 \alpha_\gamma \dfrac{\epsilon^8}{p_T^4} & \text{(a) } qq \to qq \text{ , etc.} \\ \alpha_s \alpha \dfrac{\epsilon^8}{p_T^4} & \text{(b) } gq \to \gamma q \\ \alpha_M \alpha \dfrac{\epsilon^9}{p_T^6} & \text{(c) } Mq \to \gamma_4 \end{cases} \qquad \text{(IV.2)}$$

where $\alpha_\gamma \sim \alpha/\alpha_s(p_T^2) \sim \alpha \log p_T^2/\Lambda^2$ and $\epsilon = 1-x_T$. A systematic discussion of these contributions and their relative magnitude is discussed in Ref. 2. We found that with conventional parameterizations, the CIM contributions (c) exceed the QCD (a)+(b) terms until $p_T^\gamma \sim 8$ GeV at $\sqrt{s} = 33$ GeV, and until $p_T^\gamma \sim 9$ GeV at $\sqrt{s} = 61$ GeV. The ratio of $\gamma$ to pion production (parameterized as $\epsilon^9/p_T^8$) is shown in Fig. 12. For $p_T \gtrsim 8$ GeV where the CIM subprocesses dominate both pion and photon production, we predict at $90^\circ$ the cross section ratio:[19,2]

$$\frac{\gamma}{\pi} \simeq 0.007\ p_T^2/\text{GeV}^2$$

roughly independent of $s$. This dependence of $p_T$ and $s$ should be readily distinguishable from the $\gamma/\pi \sim \alpha_\gamma/(1-x_T)$ dependence characteristic of conventional QCD calculations. We also note that the predictions of Fontannaz[41] and Blankenbecler et al.[42] which are based on the $Mq \to \gamma^* q$ subprocess appear to account for a large share of the $p_T$ distribution of massive lepton pairs.[43]

## V. Photon and Gluon Jet Production

It should be emphasized that direct large $p_T$ photon production at the

magnitude discussed here is an essential prediction of the hard-scattering approach to hadron dynamics. In particular, since photons and gluons enter subprocesses in a similar manner, there is a close relationship between gluon jet and direct photon production. For example, consider the subprocesses[11]

$$\frac{d\sigma}{dt}(gq \to gq) = \frac{\pi\alpha_s^2}{s^2}\left[-\frac{4}{9}\left(\frac{s}{u}+\frac{u}{s}\right)+\frac{s^2+u^2}{t^2}\right] \qquad (V.1)$$

and

$$\frac{d\sigma}{dt}(gq \to \gamma q) = \frac{\pi\alpha_s\alpha e_q^2}{3s^2}\left[-\left(\frac{s}{u}+\frac{u}{s}\right)\right] \qquad (V.2)$$

At 90°, this implies

$$\frac{\frac{d\sigma}{d^3p/E}(pp \to \gamma X)}{\frac{d\sigma}{d^3p/E}(pp \to gX)} = \left(\frac{1}{22}\right)\frac{\alpha}{\alpha_s(p_T^2)} \qquad (V.3)$$

from these subprocesses alone. Direct photons and gluon jets from these contributions have the same scaling laws, independent of structure functions, $k_T$ smearing, etc. We note that the $gq \to gq$ subprocess gives $\sim$1/4 of the total jet production cross section from all QCD $2 \to 2$ subprocesses.[26] Therefore we have a lower bound

$$\frac{\frac{d\sigma}{d^3p/E}(pp \to \gamma X)}{\frac{d\sigma}{d^3p/E}(pp \to \pi X)} \geq \left(\frac{\text{Jet}}{\pi}\right)_{\text{expt}} \cdot \frac{\alpha}{88\,\alpha_s(p_T^2)} \qquad (V.4)$$

For example if the jet/$\pi$ ratio is of order 300 (to 600) as in the FNAL E260 experiment[44] ($p_T \sim 4.5$ GeV, $E_{Lab} = 200$ GeV), then the $\gamma/\pi$ lower bound is 12.5% (to 25%). Conversely, the experimental upper bound for

$\gamma/\pi$ of $(.55 \pm .92)\%$ as reported by J.H. Cobb et al.[45] at $2 < p_T < 3$ GeV, $\sqrt{s} =$ 53 GeV implies an upper bound for jet/$\pi$ production of order 30, which is in severe disagreement with QCD expectations and the trend of experimental results. Thus the production of direct photons may provide one of the most important constraints on QCD subprocesses.

## VI. Color and Hadron Multiplicity

One of the most intriguing problems in QCD is how to unravel the mechanisms which control the development of hadron multiplicity in large momentum transfer reactions. The "inside-outside" space-time development of hadron production as discussed by Casher, Kogut and Susskind[46] and Bjorken[47] for $e^+e^- \to q\bar{q} \to$ hadron is consistent with causality and confinement. This picture implies that the fastest hadrons (which contain the valence quarks) are formed last, and the slow polarization cloud first. Weiss and I,[48] building on earlier work,[49] have shown that in such a picture, the charge of a quark jet (on the average) is equal to the charge of parent quark plus the average charge of anti-quarks in the sea:

$$Q_{jet} = Q_q + \langle Q_{\bar{q}} \rangle_{sea} \qquad \text{(VI.1)}$$

Here $Q_{jet}$ is obtained by integrating the charge density in the jet starting from $y_0$ (anywhere in the central region) to $Y_{max}$. Gluon jets have $Q_{jet} = 0$. These results hold for all conserved quantum numbers Q.

The inside-outside description of jet dynamics leads to the following ansatz for QCD:[3] Soft hadron production in a hard scattering reaction depends only on the effective color separation. Accordingly, two reactions which initially separate any two 3 and $\bar{3}$ systems (q, $\bar{q}$, $\bar{q}\bar{q}$, qq, etc.) will

have the same distribution of hadrons in the central region. (Only the fragmentation region discriminates the flavor and composition of the jet.) Thus we expect the same multiplicity distributions (e.g., plateau height) in the central region for the hadron system X in $e^+e^- \to X$, $\gamma^* p \to X$, and $pp \to \mu^+\mu^- + X$ (Drell-Yan mechanism), given the same rapidity separation of the 3 and $\bar{3}$ systems. For large $p_T$ reactions, the subprocess $qq \to qq$ leads to four 3 or $\bar{3}$ jets. The multiplicity and associated coherence effects associated with these jets can be computed in analogy with the soft-photon production formulas of QED for the corresponding charge separation reaction, positronium + positronium $\to e^+ + X$ [$e^+e^- \to e^+e^-$ subprocesses]. The net multiplicity corresponds to 4 quark jets, with coherent enhancement in the interference zone.

An important consequence of the color separation ansatz is that gluon (color 8) jets must have a different soft hadron spectrum than quark jets. In fact, for $N_c \to \infty$, the color separation for a gluon jet is the same as two incoherent quark jets. More generally, the number of soft gluons bremsstrahlunged from a gluon source compared to a quark source is given by the ratio of Casmir operators for the adjoint and fundamental representation:[3,4]

$$\frac{\langle n^{soft} \rangle_g}{\langle n^{soft} \rangle_q} = \frac{2}{1 - N_c^{-2}} = \frac{9}{4} \quad \text{for color SU(3)} \qquad \text{(VI.2)}$$

Thus we expect that the plateau height for soft gluons (or sea quarks) in the gluon jet is 9/4 that of quark jets (i.e., a color octet has 3/2 the "color charge" of the color triplet). If we assume that density of produced hadrons is linearly related to the sea-quark density, ther gluon jets will

have more than twice as many soft hadrons in the central region compared to quark jets. Further,[50,51] the energy of a gluon jet will be contained in a larger solid angle due to its increased "straggling" — again due to the 9/4 color factor. The leading particle distribution in a gluon jet will also be depleted more strongly by soft gluon radiation.

On the other hand the dependence of hadron multiplicity on soft gluon or quark production may not be as strong as linear. For example, the lower density of $g \to q\bar{q}$ pairs in a color triplet jet implies that the average cluster (singlet $q\bar{q}$) mass will be of higher mass than clusters due to the more copious bremsstrahlung from the color octet jet. Since the heavier clusters decay with a higher multiplicity, the net difference between quark and gluon multiplicities may not be as severe as indicated by QCD perturbation theory.[52] Nevertheless, taking into account their different structure of the short distance level, it would be very surprising if the hadron distribution from quark and gluon jets turned out to be identical.

QCD and "Hole" Partons

Several years ago Bjorken[53] postulated the concept of a "hole" parton to describe the development of the final state multiparticle distribution after a deep inelastic lepton reaction. It is an interesting question whether this parton model ansatz has an analogue in QCD.

A common phenomenological assumption is that sea quarks in a hadron arise as low-mass pair states created from gluon bremsstrahlung. If this perturbative picture is correct, then after a sea quark with rapidity $y_0$ is struck by a deep inelastic $\gamma$ or W, the spectator system consists of (1) an antiquark (hole parton) at $y \sim y_0$ with quantum numbers opposite to those of the struck quark, and (2) a leading particle system with the rapidity of

the target hadron, but with color 8 (see Fig. 13(a)). There are thus two rapidity regions created from the color neutralization: (a) a "current" plateau region of length log $Q^2$ between the 3 and $\bar{3}$, and (b) an "hadronic" plateau of length log $(W^2/Q^2)$ between the 8 and hole parton $\bar{3}$. The density of soft gluons created in the neutralization of the 8-8 system will be 9/4 that of the $3$-$\bar{3}$ separated system; thus we expect the height of the hadronic plateau to be higher than that of the current plateau; i.e., the hadronic multiplicity will be a function of both $W^2$ and $Q^2$. Despite these expectations, data from deep inelastic electron and neutrino reactions indicate that the current and hadron multiplicity plateaus have <u>equal</u> heights. We note that dual string picture also predicts that the "hadronic" plateau should be twice as high as the "current" plateau.

There is however an alternative description of the proton gluon and quark distribution, which requires giving up a simple perturbative picture of the $q\bar{q}$ sea.[54] The hadronic state is evidentally a complicated coherent color state: all constituents tend to have the same rapidity in order that the system remains a coherent singlet over the semi-infinite time before collision. The virtual gluon, quark, and anti-quark states are thus continually exchanging momentum. When a virtual sea quark is struck at $y_0$, the remaining state is that of a coherent $\bar{3}$ at the original rapidity Y of the target. Because of the exchange of momentum in the initial state, there is no special reason for a $\bar{q}$ with opposite quantum numbers to be at the struck quark rapidity, and there is no "hole" parton (see Fig. 13(b)). Furthermore, there is no separate current or hadronic plateaus; the multiplicity should only depend on log $W^2$, in agreement with data.

The question of the color and quantum number content of the hadronic state before and after a deep inelastic reaction is a fascinating subject, which deserves much more theoretical and experimental attention. The associated multiplicity in massive lepton pair production events could be an ideal laboratory for studying this problem since both valence and sea distributions of mesons and baryons can be probed, and a comparison can readily be made with either normal events or low-mass pair events.

Another important problem related to the detailed nature of the hadronic wavefunction concerns the question shadowing in deep inelastic events on nuclei. It is still not settled theoretically or experimentally whether the nucleon number $A^\alpha$ dependence is controlled by Bjorken x or $q^2$. Analyses in terms of the parton model are given in Refs. 47 and 55.

## VII. The Forward Fragmentation Region and Short-Distance Dynamics

Although hadronic scattering in the forward direction is normally not regarded as a probe of quark dynamics, the forward and backward fragmentation regions in A+B → C+X at $x_L^C \sim \pm 1$ deserves special attention. In order for C to have nearly all the momentum of A or B, there must be the exchange of large momentum transfer between constituents which are far off shell. The forward systems produced in low $p_T$ reactions can be regarded, in a general sense, as hadronic jets and many of their properties (multiplicity, $k_T$ distributions, quantum number correlations) are not dissimilar from jets in $e^+e^-$ annihilation or large $p_T$ reactions.[3] Blankenbecler and I[56] have emphasized the unity and continuity of physics throughout the Feynman plot; in particular, the dynamics at the quark and gluon level for large $p_T$ reactions at $x_R = p_C/p_C^{max} \sim 1$ at fixed $\theta_{cm}$ must connect smoothly with

forward reactions at $x_L \sim 1$ as $\theta_{cm} \to 0$ or $\pi$. In particular, Ochs[57] has noted the phenomenological similarity between particle ratios at $\theta_{cm} = 90^\circ$ and $0^\circ$ in pp collisions.

The first suggestion that the behavior of the forward fragmentation region in inclusive reactions can be related to the quark distributions in hadrons is due to H. Goldberg.[58] However, the simplest implementation of this idea fails: For example, for the reaction $pp \to \pi^+ X$, one can imagine that either before or after an initial soft scattering, a u-quark in the proton, with the distribution $G_{q/p}(x)$ (obtained from deep inelastic lepton scattering) fragments to the fast pion with the distribution $G_{\pi^+/u}$ (obtained from $e^+e^-$ annihilation) (see Fig. 14(a)). Although this ansatz can account for the observed particle ratios in the forward direction, it predicts a too-small and too-steeply falling distribution,

$$\frac{1}{\sigma}\frac{d\sigma}{dx_L}(pp \to \pi^+ X) \propto (1 - x_L)^5 \qquad \text{(prediction)}^{56} \tag{VII.1}$$

vs.

$$\frac{1}{\sigma}\frac{d\sigma}{dx_L}(pp \to \pi^+ X) \propto (1 - x_L)^{3.1 \pm 0.5} \qquad \text{(experiment)}^{59} \tag{VII.2}$$

This prediction (VII.1) can also be derived in QCD if one assumes that soft hadronic interactions are represented by gluon exchange.

There is however another possibility:[60] consider the five quark $uud\bar{q}_{sea}q_{sea}$ > component of the proton wavefunction. The sea quark has a flat distribution in rapidity and can be exchanged or annihilated in the target, giving a constant total cross section. (This is the QCD analogue of Feynman's "wee parton" mechanism for high energy interactions.) The

distribution of meson systems $u\bar{q}_{sea}$ in the remaining 4-quark state is

$$\frac{1}{\sigma}\frac{d\sigma}{dx_L}(pp \to \pi^+ X) \propto G_{\pi^+/uudd\bar{u}}(x) \sim (1 - x_L)^3 \qquad \text{(VII.3)}$$

where we have used the QCD-based spectator counting rule,[56,61]

$$G_{a/A}(x) \propto (1 - x_L)^{2n_a - 1} \qquad (x \to 1) \qquad \text{(VII.4)}$$

where $n_a$ is the number of bound spectators which are required to stop as $x = (k_0^a + k_3^a)/(p_0^A + p_3^A) \to 1$. Notice that for the gluon exchange mechanism, there are 3 spectators for $pp \to \pi^+ X$, versus 2 spectators for the sea-quark exchange case.

A large number of forward reactions have been measured; the results are generally in good agreement with the powers predicted by the q-exchange mechanisms.[60] It is likely that both soft q and g exchange mechanisms are important in forward reactions; it is just that sea quark exchange is more effective in producing fast particles. Other consequences of this picture, including induced correlations between particles at $x_L = \pm 1$ are discussed in Ref. 60. We also note that two particle correlations at $x_L(1) + x_L(2) \to 1$ are also readily predicted:

$$\frac{dN}{dx_1 dx_2}(pp \to \pi^+\pi^+ X) \sim \frac{dN}{dx_1 dx_2}(pp \to \pi^+\pi^- X) \gg \frac{dN}{dx_1 dx_2}(pp \to \pi^-\pi^- X) \qquad \text{(VII.5)}$$

where we utilize the two valence quarks in the proton. Tests of these ideas can be illuminate the multi-quark correlations in hadronic wave-functions. A recent test of the quark spectator rule for the distribution of fast forward particles in large $p_T$ reactions in correlation with various triggers has been given by the CCHK group.[62] There are also a number of successful applications of this rule to nuclear-induced reactions. An

alternative parton model for forward-fragmentation processes has been given by Das and Hwa.[63] A comparison between these approaches and applications to Drell-Yan processes is given in Ref. 64.

## VIII. Gluon Jets

The essential property of QCD which distinguishes it from a generalized quark-parton model, is the prediction of jets derived from the initial creation of a gluon quantum. Gluon jets are predicted in $e^+e^-$ annihilation (3-jet decay from $e^+e^- \to q\bar{q}g$) and in deep inelastic scattering ($eq \to eqg$). The identification of multi-jet events corresponding to such subprocesses is not completely straight-forward because of severe backgrounds from subprocesses such as $e^+e^- \to q\bar{q}q\bar{q}$; the relatively large $q \to Mq$ coupling dominates the $q \to gq$ process until quite large $p_T$. Selection of events with high multiplicity could be used to favor gluon jet production.

By comparing the processes $q\bar{q} \to \gamma+g$ and $q\bar{q} \to \mu^+\mu^-$ for high $p_T$ $\gamma$ or $\mu^+$ production, we can obtain a prediction for gluon jet production which is independent of the initial state:[65]

$$\frac{\frac{d\sigma}{d^3p/E}(AB \to \gamma X)}{\frac{d\sigma}{d^3p/E}(AB \to \mu^+ X)} = \frac{\frac{4}{3}\alpha_s(p_T^2)}{\alpha} \frac{4}{\langle \sin^2\hat{\theta} \rangle} \qquad \text{(VIII.1)}$$

Here $\sin^2\hat{\theta}$ is the subprocess center of mass production angle. Low mass $\gamma^* \to \ell\bar{\ell}$ pairs can be used here to avoid backgrounds.

The decay of heavy quark systems $Q\bar{Q}$ such as the $\Upsilon$ into 3 gluons[5] or $\gamma$+2 gluons[6] could provide the cleanest test of QCD gluon jet phenomenology. The standard perturbation formulae for positronium decay, updated for color

factors gives the branching ratio[66]

$$\frac{\Gamma(\Upsilon \to \gamma gg)}{\Gamma(\Upsilon \to ggg)} \simeq \frac{36}{5}\left(\frac{e_Q}{e}\right)^2 \frac{\alpha}{\alpha_s(M_\Upsilon^2)} \qquad \text{(VIII.2)}$$

where $Q^2 \simeq M_\Upsilon^2$ is the effective off-shell value to be used in the running coupling constant. If $e_Q = 1/3$, the branching ratio is 3%. Predictions for the angular distributions of the $\Upsilon$ decay plane relative to the beam axis and decay distributions are given in Ref. 6. The $\Upsilon \to \gamma gg$ two-jet channel is particularly interesting since the $gg \to \Lambda$ mass can be varied and a direct comparison with SPEAR $q\bar{q}$ jets at the same energy can be made. The predicted spectrum based on perturbation theory as a function of $M_{gg}^2 = M_\Upsilon^2 (1-x_\gamma)$, $x_\gamma = p_\gamma/p_{max}$, is shown in Fig. 15. Resonances with the gg quantum numbers ($\eta$, $\eta'$, $\eta_c$, glue-balls) can be expected to modulate the perturbative prediction over a local region if we assume local duality.

It should be noted that all of these predictions for gluon jet production treat the gluon as strictly massless. Although this is evidently correct for QCD matrix elements, the fact that the gluon "decays" to a massive jet may indicate that we should include mass spectrum effects and thresholds in the phase space calculations. Such effects could distort simple QCD predictions; e.g., the $\Upsilon \to \gamma gg/ggg$ ratio will be enhanced. We also note that higher order (in $\alpha_s$) channels $\Upsilon \to gq\bar{q}$ and $q\bar{q}$ could be relatively more important than indicated by perturbation theory if the gluon jet has an effectively heavier mass spectrum than the quark jet.[68]

To summarize, let us list the discriminants which could distinguish quark and gluon jets:

(a) Multiplicity. As discussed in Section VI, color octet separation leads to multiplicity of soft gluons and sea quarks 9/4 as large as color triplet separation.[3,4] If this translates into higher hadron multiplicity, then $\Upsilon \to 3g$ decay events with low sphericity will have a higher rapidity plateau in the central region with respect to the $g + (gg)$ jet axis.

(b) Leading particles. If we trust lowest order QCD perturbation theory, then the distribution of charged particles at $x \to 1$ falls off faster in gluon jets compared to hadron jets. A simple form which has the predicted $x \to 0$ and $x \to 1$ limiting behavior is[3,69]

$$D_{H^{\pm}/g}(x) \approx \frac{9}{8}\left[D_{H/q}(x) + D_{H/\bar{q}}(x)\right](1-x) \qquad \text{(VIII.3)}$$

Gluon jets, however, may have enhanced number of $I = 0$ states at $x \to 1$ which have a strong gluon component, e.g., $g \to \eta, \omega, \psi$, etc.[70]

(c) Quantum numbers. The total charge of the jet in its fragmentation region is related to the charge of the parent as discussed in Section VI.

(d) Transverse momentum distribution. Gluon jets should be more diffuse (large $\langle k_T^2 \rangle$) than quark jets because of the increased number of soft gluon interactions (increased "straggling").[50,51,7] This effect also results if the gluon decays to $q\bar{q}$ before color neutralization occurs.

(e) Gluon jets may be "oblate." It is possible that the (linear) polarization of a gluon is reflected by the distribution of hadrons in the jet. This possibility is discussed in detail in a recent paper by DeGrand and Schwitters and myself.[7]

For example, suppose that hadrons are produced from gluon jets after the decay $g \to q\bar{q}$. Then by convolution,

$$G_{H/g}(z,\phi) \approx \int_z^1 \frac{dx}{x} G_{H/q}\left(\frac{z}{x}\right) G_{g/q}(x,\phi) + (q \to \bar{q}) \quad . \qquad \text{(VIII.4)}$$

In lowest order perturbation theory spin 1/2 quarks from $g \to q\bar{q}$ are aligned with respect to the gluon linear polarization:

$$G_{q/g}(x,\phi) \propto [1 - 4\cos^2\phi\, x(1-x)]$$

$$\cos\phi = \hat{q} \cdot \hat{\epsilon} \qquad \text{(VIII.5)}$$

This then implies a sum rule for the momentum weighted distribution of hadrons:

$$\frac{d\Sigma}{d\phi} \equiv \sum_H \int_0^1 dz\, z\, D_{H/g}(z,\phi)$$

$$= \frac{1}{4\pi}(1 + 2\sin^2\phi) \quad . \qquad \text{(VIII.6)}$$

In this model, hadrons are 3 times more likely to be produced orthogonal rather than parallel to $\hat{\epsilon}$, thus producing a non-cyclindrical "oblate" jet. Oblateness can be determined experimentally by finding the principal axes of $\sum_H p_i^H p_j^H$ as in sphericity analyses.

Equation (VIII.6) should be regarded as an upper limit to the oblateness effect in QCD, since (1) not all hadrons arise from the q and $\bar{q}$ decay products, and (2) the "straggling" from $g \to g_{soft} + g$ due to soft gluon emission depolarizes the gluon. The latter effect is of order $\alpha_s(s)$ and can probably be diminished by selecting events with fast hadrons. The main problem is that gluons are not produced 100% linearly polarized in a given direction.

For example, in $\eta(Q\bar{Q}) \to g + g \to q\bar{q} + q\bar{q}$ (pseudoscalar decay analogue of $\pi^0$ double Dalitz decay), the correlation between gluon polarizations is

$$\frac{dN}{d\psi} = \frac{1}{9\pi}(4 + \sin^2\psi) \qquad \text{(VIII.7)}$$

and

$$\frac{d\epsilon}{d\psi} \equiv \sum_{H_a,H_b} \int_0^1 dz_a \int_0^1 dz_b \; \frac{dN}{dz_a\, dz_b\, d\phi}\, z_a\, z_b$$

$$= \frac{15 + 2\sin^2\psi}{32\pi} \qquad \text{(VIII.8)}$$

gives the summed correlation between hadrons of the two jets. The maximal effect is only 13%. Similarly in $\Upsilon \to 3q$, the polarization of each gluon is correlated with the normal to the decay plane. Summing over hadrons (from $g \to q\bar{q} \to$ hadrons + $q + \bar{q}$) gives

$$\frac{d\epsilon}{d\chi} = (X_1^2 + X_2^2 + X_3^2) + \frac{1}{4}(1 - 2\cos^2\chi)\, X_1\, X_2\, X_3 \qquad \text{(VIII.9)}$$

where $\cos\theta_{23} = 1 - X_1$ is the cosine of the angle between the gluon jets, and $\cos\chi = p_{\hat{H}} \cdot \hat{n}$ is the projection of the hadron direction with the decay plane normal. The maximal effect occurs for $\theta_{ij} = 120^\circ$ ("tripod" configuration), where we predict that a hadron is 9/7 more likely to be aligned in the plane than normal to the plane.

Finally, for $e^+e^- \to q\bar{q}g$ or $eq \to eq'g$ events, the distribution of gluon polarization is given by

$$z\,\frac{dN}{dz\,d\phi\,d^2k_T} = z\,G_{g/q}(z,\phi,\vec{k}_T^2) \sim \frac{4}{3}\frac{\alpha_s}{\pi^2}\left[z^2 + 4(1-z)\cos^2\phi\right]\frac{\vec{k}_T^2}{(\vec{k}_T^2 + z^2 m_q^2)^2} \qquad \text{(VIII.10)}$$

where $\cos\phi = \hat{\epsilon} \cdot \hat{n}$ and $\hat{n}$ is in the plane of $q\bar{q}$ or $qq'$. The average over $\phi$ gives the standard $1 + (1-z)^2$ distribution.

Although these model calculations give only a first estimate, it seems likely that the spin-1 nature of the gluon in QCD will be reflected in the oblateness of the distribution of its decay products.

## IX. The Gluon Distribution in Hadrons[8]

Another important question concerning the hadron wave function is the nature of its gluon distribution. In QCD, there are three essentially different sources of gluons within a meson or baryon.

(a) The gluon induced by a scattering process. As in QED, these are the quanta associated with changing the momentum of color sources; the charge in the color field generates bremsstrahlung along the initial and final directions. These gluons (and their associated $q\bar{q}$ sea quark pairs) yield the scale-breaking and moments of QCD radiative corrections in deep inelastic processes.

(b) The gluons associated with the exchange interactions and the binding potential. These gluons are target-dependent and cannot be identified with a single quark line.

(c) The gluons which are constituent fields of the hadron. These gluons are non-perturbative, and on-average tend to have the same rapidity as the hadron bound state. Again, they are target-dependent and cannot be associated with a single quark line.

For $x \to 1$, the gluon distribution from sources (a) and (b) fall one power faster than the quark distribution, if QCD perturbation theory can be taken as a guide:

$$\text{(a),(b):} \quad \begin{cases} G_{g/p} \sim (1-x)\, G_{q/p} \sim (1-x)^4 \\ G_{\bar{q}/p} \sim (1-x)^5 \end{cases} \qquad x \to 1 \qquad \text{(IX.1)}$$

In addition there are $q^2$-dependent radiative corrections from soft gluon emission from the gluon or quark which modify these powers, as in the analysis of DDT.[30] The distribution of gluons at $x \to 1$ from source (c),

can be computed from the spectator counting rule.[56] For the <qqqg> Fock state, there are 3 quark spectators, yielding

$$(c): \begin{cases} G_{g/p}(x) \sim (1-x)^6 \\ G_{q/p}(x) \sim (1-x)^7 \end{cases} \qquad x \to 1 . \qquad \text{(II.2)}$$

The observed distribution can be expected to be a linear combination of these sources.

Thus far only gluons from quark bremsstrahlung (type (a)) have been taken into account in the standard QCD phenomenological analyses:[71] one assumes that at some $Q_0^2$ the proton only consists of valence quarks, and that the gluons and sea quarks can be generated by QCD evolution equations for $Q^2 \neq Q_0^2$. In such an approach the probability distribution for quarks is sufficient to determine the probability distribution for gluons. Only "diagonal" terms are computed; off-diagonal diagrams involving two quarks are not considered. This analysis reproduces the $q^2$-dependent QCD moments for structure functions.

However, for x and $\vec{k}_T \to 0$ (the long wavelength limit) the gluon only "sees" a color singlet source; thus there must be coherent cancellations between the different quark currents. The diagonal approximation can only be accurate for large transverse momentum gluons (see Fig. 16).

Gunion and I[7] have recently considered a simple gauge theory model of the meson which preserves gauge invariance and allows a detailed study of the color coherence effects. (The same physics also occurs in QED when one determines the photon distribution in a neutral atom, such as positronium). In the model, the gluon distribution can be computed in lowest order analytically for all x and $k_T$. For small x, we find

$$G_{g/M}(x,\vec{k}_T^2) = \frac{8}{3}\frac{\alpha_s}{\pi^2}\frac{1}{x}\frac{1}{\vec{k}_T^2}\left[1 - F_M\left(\frac{\vec{k}_T^2}{(1-\bar{x}_q)^2}\right)\right] \qquad \text{(IX.3)}$$

where $F_M(Q^2) \simeq 1/(1 + Q^2/M_V^2)$ is the meson electromagnetic form factor. The first term in the bracket is the usual (diagonal) contribution obtained from the convolution of $G_{q/M}$ or $G_{\bar{q}/M}$ with $G_{g/q}$. The $F_M$ term from the (off-diagonal) coherence of the q and $\bar{q}$ distributions is only unimportant at large $k_T^2 \gg (1-\bar{x}_q)^2 M_V^2$, where $\bar{x}_q \simeq 1/2$ is the average momentum fraction of the quark in the meson, and $M_V$ sets the scale of the electromagnetic form factor and hadron size. The coherence of the color singlet bound state eliminates the usual infrared divergences at $\vec{k}_T^2 \to 0$. In this simple model, the standard denominator for a quark target $(\vec{k}_T^2 + x^2 m_q^2)^{-1}$ is replaced by $(\vec{k}^2 + M_V^2)^{-1}$; i.e., there is no quark mass singularity for $m_q \to 0$.

The most important consequence for phenomenology is the fact that the gluon distribution in a hadron reflects its size and constituency. The gluon momentum and sea quark fractions will be bigger the larger the size (# of the hadron $\left(xG_{g/h}(x) \sim \log\left(1 + \lambda_H^2 k_{Tmax}^2\right)\right)$. In addition, the gluon distribution in a hadron clearly tends to increase with the number of quark constituents. Eventually, at large enough $\log q^2$ the QCD radiative corrections will cause the structure functions to contract to the $x \sim 0$ region, and the gluon and quark momentum fractions will reach an asymptotic equilibrium independent of the nature of the target. However, in the preasymptotic domain, target effects are important for determining the gluon and sea-quark distributions. A number of applications are discussed in Ref. 7 including the prediction that the gluon momentum fraction in mesons at present $q^2$ is appreciably smaller than in nucleons. This prediction can be tested in reactions such as $\phi$ production

or gluon jet production in hadronic collisions, where a gluon-induced subprocess is expected to play a major role.[72]

The models used thus far for the gluon distribution in hadrons are primitive and can only take into account perturbative effects. Non-perturbative calculations which can account for final state interaction effects, and higher Fock state components in the bound state wavefunction will be required before a definitive prediction of the gluon distribution in a hadron can be made.

## X. Conclusions

Although there are tantalizing hints of success, there is as yet no convincing quantitative evidence that inclusive hadronic reactions are described by perturbative quantum chromodynamics. A great deal of experimental and theoretical work will be required to provide bona fide tests of the theory at even the 10-20 percent level. Among the outstanding problems:

(1) The production cross section for jets in hadron-hadron collisions is not known to within a factor of 2 or 3, let alone its scaling properties at fixed $x_T$ and $\theta_{cm}$. If the combined QCD plus CIM description given here is correct the jet/$\pi$ cross section should increase as $\sim p_T^2$ at fixed $x_T$ and $\theta_{cm}$ for $p_T \gtrsim 4$ GeV/c. The inclusive jet cross section from perturbative QCD is predicted to scale as

$$E_J \frac{d}{d^3 p_J} (pp \to \text{Jet} + X) \sim \frac{\alpha_s^2 (p_T^2)}{p_T^4} f(x_T, p_T, \theta_{cm}) \qquad (X.1)$$

where f includes the logarithmic scale breaking from the structure functions:

$$f(x_T, p_T, \theta_{cm}) \underset{\substack{\theta_{cm} = 90^\circ \\ x_T \sim 1}}{\sim} (1 - x_T)\, G^2_{q/p}\,(x_T, p_T^2) \qquad (X.2)$$

where

$$G_{q/p}\,(x_T, p_T^2) \sim (1 - x_T)^{3 + \tilde{\xi}(p_T^2)} \qquad (X.3)$$

$$\tilde{\xi}(p_T^2) = \frac{4}{3\pi} \int_{\mu^2}^{p_T^2} \frac{dt^2}{t^2}\, \alpha_s(t^2) \sim \log \log\,(p_T^2) \qquad (X.4)$$

gives the scale-breaking of the proton structure function due to QCD radiative corrections. The $k_T$ smearing effect for $p_T > 4$ GeV/c changes the predictions by less than a factor of 2 if off-shell kinematics are used.[18]

(2) The existence of charge correlations between the trigger and away side hadrons, as observed by the BFS collaboration[25] evidentally eliminate 2 to 2 QCD Born subprocesses as the dominant hard scattering mechanism for single hadron production in the region up to $p_T > 4$ GeV. The extension of these measurements to higher $p_T$ and $x_T$ is critical. Nuclear targets tend to obscure flavor correlations because of charge averaging and final state interactions.

(3) Cross sections for hadron pairs at large $M^2$ tend to be insensitive to the controversial $k_T$ smearing effect. It is particularly interesting to compare hadron pairs and muon pairs at the same kinematics. One predicts[73]

$$\frac{\frac{d\sigma}{dM^2 dy}\,(pp \to H^+H^-X)}{\frac{d\sigma}{dM^2}\,(pp \to H^+H^-X)} = \left(\frac{1}{M^2}\right)^k f\left(y, \frac{M^2}{s}\right) \qquad (X.5)$$

where $k = 2$ for meson pairs and $k = 4$ for baryon pairs. If 2 to 2 QCD diagrams are dominant, then $k = 0$, and there are only minor scale violations from the relevant structure functions and an overall factor of $\left[\alpha_s(M^2)/\alpha\right]^2$.

(4) It is very important that QCD predictions for direct high $p_T$ photon reactions be tested, starting with the original Bjorken-Paschos[74] inelastic Compton reaction $\gamma p \to \gamma X$ and inclusive photoproduction $\gamma p \to \pi X$ (reactions without forward hadrons) to direct photon production $pp \to \gamma X$, two photon processes $\gamma\gamma \to X$, $e^+e^- \to \gamma + \pi^\pm + X$ (charge asymmetry), and $e^\pm p \to e^\pm \gamma X$ ($\pi^\pm$ asymmetry).[40] The photon is the only non-colored elementary field that directly participates in QCD dynamics at short distances; unless its pointlike couplings to quarks are confirmed, predictions for perturbative processes involving gluons are probably meaningless. The close relationship between photon production to gluon and quark jet production is discussed in Section V. We also note the remarkable fact that the asymptotic photon structure function is scale-invariant up to an overall factor of $\alpha_s^{-1}(p_T^2)$, and photon-induced cross sections such as $Ed\sigma/d^3p$ ($\gamma\gamma \to$ Jet + X) are asymptotically scale free and independent of $\alpha_s(p_T^2)$ when perturbative contributions to all orders are included.[1,38]

(5) The complete picture of quark and gluon distributions in hadrons will require attention to coherent effects and multiparticle correlations, as discussed in Section IX. Measurements of the final states in deep inelastic processes and massive lepton pair production processes, together with comparisons with low $q^2$ and low $M^2$ events, can give detailed information on the evolution of multiquark and gluon jets, including the effect of color separation, "hole" parton production, and the influence of nuclear targets.

(6) Surprisingly, the most convincing evidence for underlying scale-invariant quark interactions comes from large momentum transfer exclusive measurements such as the form factors at large t and hadron scattering and photoproduction at large t and u. For example, the fact that large t data for $t^2F_{1p}(t)$ and $tF_\pi(t)$ are consistent with constant behavior indicates that the proton and pion can be described as qqq and $q\bar{q}$ bound states with internal interactions appropriate to renormalizable (but not fixed point) field theories.[14] The effects of asymptotic freedom corrections on exclusive large momentum transfer exchange processes is presently under study.[32] Much more experimental and theoretical work on the spin[76] and angular dependence of these processes is required before we can obtain a detailed understanding of the possible QCD mechanisms responsible for exclusive hadron interactions at short distance.

## ACKNOWLEDGEMENTS

A large part of this talk is based on collaboration with R. Blankenbecler, W. Caswell, T. DeGrand, J. Gunion, R. Rückl, R. Schwitters, J. Weis, and N. Weiss. It is a pleasure to thank them and also J. Bjorken, C. Carlson, J. Ellis, R. Field, P. Lepage, Y. Frishman, K. Hansen, P. Scharbach, and D. Sivers for helpful conversations.

## REFERENCES


1. S. J. Brodsky, T. DeGrand, J. F. Gunion, and J. Weis, Phys. Rev. Lett. 41, 672 (1978), and SLAC-PUB-2199 (submitted to Phys. Rev.).
2. R. Ruckl, S. J. Brodsky, and J. Gunion, SLAC-PUB-2115 (to be published in Phys. Rev.).

   F. Halzen and D. Scott, Phys. Rev. Lett. 40, 1117 (1978).

   H. Fritzsch and P. Minkowski, Phys. Lett. 63B, 99 (1976).
3. S. J. Brodsky and J. F. Gunion, Proc. of the 7th Int. Coll. on Multiparticle practions, Munich (1976), Phys. Rev. Lett. 37, 402 (1976).
4. K. Konishi, A. Ukawa, and G. Veneziano, CERN-TH-2509 (1978).
5. T. DeGrand, Y. J. Ng, and S.-H. H. Tye, Phys. Rev. D16, 3251 (1977).

   K. Koller, H. Krasemann, and T. F. Walsh, DESY 78137 (1978).

   K. Koller and T. Walsh, 781/6 (1978).

   A. DeRujula, J. Ellis, E. G. Floratos, and M. K. Gaillard, CERN preprint TH-2455 (1978).
6. S. J. Brodsky, D. G. Coyne, T. A. DeGrand, and R. R. Horgan, Phys. Lett. 73B, 203 (1978).

   M. Kramer and H. Krasemann, Phys. Lett. 73B, 58 (1978).
7. S. J. Brodsky, T. A. DeGrand, and R. F. Schwitters, SLAC-PUB-2160 (1978), to be published in Phys. Lett.
8. S. J. Brodsky and J. F. Gunion, SLAC-PUB-2163 (1978).
9. D. Sivers, R. Blankenbecler, and S. J. Brodsky, Phys. Reports 23C:1 (1976).

   M. Jacob and P. V. Landshoff, to be published in Phys. Reports.

10. R. D. Field, CALT-68-683 (presented at the XIX Int. Conf. on High Energy Phys., Tokyo, 1978, and references, therein).

11. R. Cutler and D. Sivers, Phys. Rev. D16, 679 (1977); Phys. Rev. D17, 196 (1978).

B. L. Combridge, J. Kripfganz, and J. Ranft, Phys. Lett. 234 (1977).

12. R. Blankenbecler, S. J. Brodsky, and J. F. Gunion, Phys. Rev. D18, 900 (1978).

P. V. Landshoff and J. C. Polkinghorne, Phys. Rev. D8, 927 (1973). Phys. Rev. D10, 891 (1974).

13. We cavalierly refer to subprocesses which involve more than the minimum number of external fields as "high twist."

14. S. J. Brodsky and G. Farrar, Phys. Rev. D11, 1309 (1975).

15. Note, however that the standard QCD corrections to the structure functions $G_{a/A}(x,Q^2)$ depend on the color Casmir operators of a and thus vanish if the constituent is a color singlet.

16. S. D. Ellis, M. Jacob, and P. V. Landshoff, Nucl. Phys. B108, 93 (1976). See also J. D. Bjorken and G. R. Farrar, Phys. Rev. D9, 1449 (1974).

17. P. V. Landshoff, J. C. Polkinghorne, and R. D. Short, Nucl. Phys. B28, 222 (1971).

S. J. Brodsky, F. E. Close, and J. F. Gunion, Phys. Rev. D8, 3678 (1973).

18. For an extensive discussion see W. F. Caswell, R. R. Horgan, and S. J. Brodsky, SLAC-PUB-2106 (to be published in Phys. Rev.). Detailed calculations for QCD subprocesses are given by R. R. Horgan and P. Scharbach, SLAC-PUB-2188 (1978). The importance of off-shell

kinematics in calculating $k_T$ fluctuations has also been discussed by K. Kinoshita and Y. Kinoshita, KYUSHU-78-HE-6 (1978), M. Chase, DAMTP 77/29 (1977), R. Raitio and R. Suanowski, HU-TFT-77-22 (1977).

19. R. Blankenbecler, S. J. Brodsky, and J. F. Gunion, Ref. 12, and Phys. Rev. D6, 2652 (1972).

20. S. J. Brodsky and G. Farrar, Phys. Rev. Lett. 31, 1/53 (1973). V. A. Matveev, R. M. Muradyan, and A. N. Tavkhelidze, Lett. Nuovo Cimento 7, 719 (1973).

21. D. Antreasyan, et al., preprint EFI 78-29 (1979), Phys. Lett. 38, 112 (1977); J. W. Cronin, et al., Phys. Rev. D11, 3105 (1975). See also M. Shochet, Proc. of the XVIII Int. Conf. on High Energy Phys., Tbilisi (1976).

22. A. G. Clark, et al., Phys. Lett. 74B, 267 (1978). CERN-Columbus-Oxford-Rockefeller Expt., reported by L. Di Lella in Workshop on Future ISR Phys., Sept. (1977), edited by M. Jacob.

23. D. Jones and J. F. Gunion, SLAC-PUB-2157 (1978).

24. R. P. Feynman, R. D. Field, and G. C. Fox, Nucl. Phys. B128, 1 (1977). R. D. Field and R. P. Feynman, Phys. Rev. D15, 2590 (1977). R. Baier, J. Cleymans, K. Kinoshita, and B. Peterson, Nucl. Phys. B118, 139 (1977). J. Kripfganz and J. Ranft, Nucl. Phys. B124, 353 (1977).

25. M. G. Albrow, et al., NBI preprints (1978), presented by R. Møller to this conference, and K. H. Hansen, presented to the XIX Int. Conf. on High Energy Phys., Tokyo (1978), and Nucl. Phys. B135, 461 (1978).

26. R. P. Feynman, R. D. Field, and G. C. Fox, CALT-68-651 (1978). See also A. P. Contogouris, R. Gaskell and S. Papadopoulos, Phys. Rev. D17, 2314 (1978), A. P. Contogouris, McGill preprint (1978). J. F.

Owens and J. D. Kimel, FSU HEP 780330 (1978), J. F. Owens, FSU HEP 780609 (1978), Phys. Lett. 76B, 85 (1978).

J. Ranft and G. Ranft, preprints KMU-HEP-7806 and 7805 (1978), Nuovo Cimento Lett. 20, 669 (1979).

M. Fontannaz, Nucl. Phys. B132, 452 (1978).

27. A Simplified analysis of charge correlations is given in S. J. Brodsky, Proc. of the VII Int. Symp. on Multiparticle Dynamics, Kayserberg, France, June (1977). An analysis of the QCD Born subprocesses is given by R. P. Feynman, et al., Ref. 26.

28. R. J. Fisk, et al., Phys. Rev. Lett. 40, 984 (1978).

29. J. D. Bjorken and J. B. Kogut, Phys. Rev. D8, 1341 (1973).

30. Y. L. Dokshitser, D. I. Dyakonov, and S. I. Troyan, SLAC-TRANS-0183, Trans. from Proc. of the 13th Leningrad Winter School on Elementary Particle Phys. (1978); Leningrad preprint (1978).

31. J. C. Vander Velde, this conference; J. S. Bell, et al., UMBC-9 (1978).

32. S. J. Brodsky, G. P. Lepage, and Y. Frishman (to be published).

33. J. C. Polkinghorne, Phys. Lett. 49B, 277 (1974).

34. J. M. Cornwall and G. Tiktopoulos, Phys. Rev. D13, 3370 (1976); D15, 2937 ('977).

35. H. Terazawa, Rev. Mod. Phys. 43, 615 (1973).

V. M. Budnev, et al., Phys. Reports 15C (1975).

S. J. Brodsky, T. Kinoshita, and H. Terazawa, Phys. Rev. D4, 1532 (1971).

36. See also the recent papers of C. H. Llewyllyn Smith, Oxford preprint 56/78 (1978) and K. Kajantie, Helsinki preprint HU-TFT-78-30 (1978). The first calculation of the $\gamma\gamma \to q\bar{q}$ process for single hadron production was given by J. D. Bjorken, S. Berman, and J. Kogut, Phys. Rev. D4,

3388 (1971). A discussion for virtual γ reactions is given by T. F. Walsh and P. Zerwas, Phys. Lett. 44B, 195 (1973).

37. F. Witten, Nucl. Phys. B120, 189 (1977).
W. Frazer and J. F. Gunion, UCSD preprint 10P10-194 (1978).
C. H. Llewyllin Smith, Ref. 36.

38. This scaling property was first pointed out in Ref. 36.

39. This point has been emphasized by W. Ochs and L. Stodolsky (unpublished).

40. See Ref. 2, C. O. Escobar, DAMTP 78/9 (1978).
G. R. Farrar and S. C. Frautschi, Phys. Rev. Lett. 36, 1017 (1976).
J. D. Bjorken, et al., Ref. 36.
An indication that the interactions of large transverse moment real photon have point-like interactions is given by the measurements of the $e^+ - e^-$ asymmetry is deep inelastic bremsstrahlung by D. L. Fancher, et al., Phys. Rev. Lett. 38, 800 (1977). See also S. J. Brodsky, J. F. Gunion, and R. L. Jaffe, Phys. Rev. D6, 2487 (1972).

41. M. Fontannaz, Phys. Rev. D14, 3127 (1976).

42. M. Duong-van, K. V. Vasavada, and R. Blankenbecler, Phys. Rev. D16, 1389 (1977).

43. C. M. Debeau and D. Silverman (to be published) have given a combined QCD + CIM calculation of the massive lepton pair transverse momentum distribution.

44. C. Bromberg, et al., Phys. Rev. Lett. 38, 1447 (1977), Nucl. Phys. B134, 189 (1978).
M. D. Corcoran, et al., presented at the XIX Int. Conf. on High Energy Phys., Tokyo (1978).

45. J. K. Cobb, et al., CERN preprint 78-0925 (1978).

46. A. Casher, J. Kogut, and L. Susskind, Phys. Rev. Lett. 31, 792 (1973).

47. J. Bjorken, SLAC-PUB-1756, Lectures given at the Int. Summer School in Theor. Phys., DESY (1975).

48. S. J. Brodsky and N. Weiss, Phys. Rev. D16, 2325 (1977).

49. G. R. Farrar and J. Rosner, Phys. Rev. D7, 2747 (1973).
J. L. Newmeyer and D. Sivers, Phys. Rev. D9, 2592 (1974).
R. Cahn and E. Colglazier, Phys. Rev. D9, 2592 (1974).

50. K. Shizuya and S.-H. H. Tye, FermiLab-PUB-78/54 (1978).

51. M. Einhorn and B. Weeks, SLAC-PUB-2164 (1978).

52. A. Casher, H. Neuberger, and S. Nussinov, Tel Aviv preprint TAUP-694-78 (1978).

53. J. Bjorken, Phys. Rev. D7, 282 (1973).

54. See Refs. 3, 19, and 48.

55. S. J. Brodsky, J. F. Gunion, and J. Kuhn, Phys. Rev. Lett. 39, 1120 (1977).

56. S. J. Brodsky and R. Blankenbecler, Phys. Rev. D10, 2973 (1974).

57. W. Ochs, MPI-PAE/PTH 33/77 (1977), Proc. of the 12th Rencontre de Moriond, Flaine (1977), Nucl. Phys. B118, 397 (1977).

58. H. Goldberg, Nucl. Phys. B44, 149 (1972).

59. J. C. Sens, et al., CHLM Colloboration (unpublished).

60. S. J. Brodsky and J. F. Gunion, Phys. Rev. D17, 848 (1978).

61. If the spin of the leading particle does not match that of the projectile, there is an additional suppression factor $(1-x)^{2|s_g^a - s_g^A|}$. S. Brodsky, J. Gunion, N. Fuchs, and M. Scadron (to be published).

62. E. E. Kluge, et al. (CCHK collaboration), this conference; D. Drijard, et al., CERN/EP/Phys. 78-14 (1978).

63. K. P. Das and R. C. Hwa, Phys. Lett. 68B, 459 (1977); 73B, 504 (1978).

64. T. A. DeGrand and H. I. Miettinen, Phys. Rev. Lett. 40, 612 (1978).
T. A. DeGrand, SLAC-PUB-2182 (1978).

65. S. J. Brodsky, W. Caswell, and R. Horgan (unpublished), see S. J. Brodsky, SLAC-PUB-1937, Proc. of the 12th Recontre de Moriond, Flaire (1977).

66. M. Chanowitz, Phys. Rev. D12, 918 (1975).
L. Okun and M. Voloshin, ITEP-95 (1976).

67. V. A. Novikov, et al., Phys. Report 41C, 1 (1978).

68. S. J. Brodsky, M. Dine, and E. Fahri (in progress).

69. S. J. Brodsky, Ref. 65.

70. H. Fritzsch and K. H. Streng, CERN-TH-2520 (1978).

71. See, e.g., A. Buras and K. Gaemar, Nucl. Phys. B132, 249 (1978).
For a detached discussion of the diagonal approach see F. Martin, SLAC-PUB-2192 (1978).

72. S. Ellis and M. Einhorn, Phys. Rev. D12, 2007 (1975); Phys. Rev. Lett. 36, 1263 (1976).
C. Carlson and R. Suaya, Phys. Rev. D14, 3115 (1976); Phys. Rev. D18, 760 (1978).

73. R. Blankenbecler and S. J. Brodsky (unpublished).

74. J. D. Bjorken and E. Paschos, Phys. Rev. 185, 1975 (1969).

75. S. J. Brodsky, G. P. Lepage, Y. Frishman (in progress).

76. QCD-based reductions for the spin-dependence of exclusive reactions is given by G. R. Farrar and C-C. Wu, Nucl. Phys. B85 (1978), S. J. Brodsky, C. Carlson, and H. Lipkin (to be published), and G. R. Farrar, S. Gottlieb, D. Sivers, and G. Thomas (to be published).

## FIGURE CAPTIONS

1. QCD hard scattering subprocesses for $pp \to \pi X$. In (a), (b), and (c) the $\pi$ is formed after the hard scattering via quark or gluon fragmentation. In (d) and (e), the "higher twist" CIM contributions, the meson is formed before the hard scattering. Diagram (f) represents the "fusion" CIM $q\bar{q} \to \pi + M$ contribution.

2(a). Data and QCD contributions for $Ed\sigma/d^3p$ $(pp \to \pi X)$ at $\theta_{cm} = 90^\circ$. The dotted line has no scale violations or $k_T$ fluctuations. The lower solid curve indicates scale violations in the structure functions and $\alpha_s$. The upper solid curve indicates scale violations plus $k_T$ fluctuations calculated with off-shell kinematics.

(b). QCD results for $p_T^8\, Ed\sigma/d^3p$ $(pp \to \pi^0 X)$. The dashed curves indicates scale violations. The solid curves indicate scale violations plus off-shell $k_T$ fluctuations. (From Horgan and Scharbach, Ref. 18.) The sum of QCD plus CIM diagrams give a good fit to the data. See Figs. 5 and 8.

3. Contribution of $qM \to qM$ amplitude (a) to meson-baryon scattering (b) and the meson form factor (c).

4. The CIM $Mq \to \pi q$ contribution to $pp \to \pi X$ at large $p_T$. The virtual meson M is a $q\bar{q}$ component of the nucleon.

5. Comparison with data of CIM plus QCD $(p_T^{-4})$ contributions to the $pp \to \pi^0 X$ cross section. Scale-breaking is neglected and $\alpha_s = .15$ in the QCD term. (From Jones and Gunion, Ref. 23.)

6. Analyses of charge flow in CIM diagrams for $pp \to K^{\pm} X$. Quark exchange in the subprocess implies charge correlations between the trigger and away side jet.

7. Number of fast positive and negative particles on the side away from a $90^{o}$ trigger for various trigger type. (From Ref. 25.) The gluon exchange QCD diagrams give an away side jet nearly independent of the trigger type. See R. Field, Ref. 10.

8. Comparison with data of CIM plus QCD ($p_T^{-4}$) contributions to the $pp \to \pi^{o}X$ cross section. Scale-breaking is neglected and $\alpha_s = .15$ in the QCD term. (From Jones and Gunion, Ref. 23.) The data may include contributions from direct photons, $pp \to \gamma X$.

9. Illustration of hard scattering expansion. The Feynman amplitude (a) contains contributions from (a) $qq \to qq$, and (b) $gq \to gq$ subprocesses.

10. (a) Two photon collisions in $e^{\pm}e$ interactions. Jet production from (b) $\gamma\gamma \to q\bar{q}$, (c) $\gamma q \to gq$, and (d) $qq \to qq$ subprocesses.

11. Cross section $p_T^4\, Ed\sigma/d^3p$ ($\alpha\alpha \to$ Jet + X) at $\sqrt{s} = 30$ GeV from $\gamma\gamma$ subprocesses: (a) $\gamma\gamma \to q\bar{q}$, (b) $\gamma\gamma \to Mq\bar{q}$, (c) $\gamma\gamma \to q\bar{q}g$, (d) $\gamma\gamma \to q\bar{q}\ q\bar{q}$, (e) $\gamma\rho \to q\bar{q}$, and (f) $\gamma\gamma \to M\bar{M}\ q\bar{q}$. The dotted line gives the sum.

12. Predicted ratio from QCD plus CIM contributions for $\gamma/\pi$ in pp collisions. (From F. Rückl et al., Ref. 2.)

13. Illustration of final state hadron distribution deep inelastic lepton scattering on a sea quark arising from (a) gluon bremsstrahlung or (b) a $(q\bar{q}\ qqq)$ rock state.

14. Production of high energy, low $p_T$ pions in $pp \to \pi^{+}X$ arising from (a) diffractive or gluon exchange processes or (b) $q\bar{q}$ annihilation of sea quarks.

15. Decay distributions for $\chi \to \gamma + X$ in $x = 2q/M_\chi$ and $M_X^2/s$ from the simplest QCD diagrams $\chi \to g+g+\gamma$, and massless gluons. The modulation of a singlet resonance at fixed $M_X^2$ is shown schematically.

16. Contributions to quark sea from (a) diagonal, and (b) off-diagonal gluon contributions. Only (a) is considered in usual analyses.

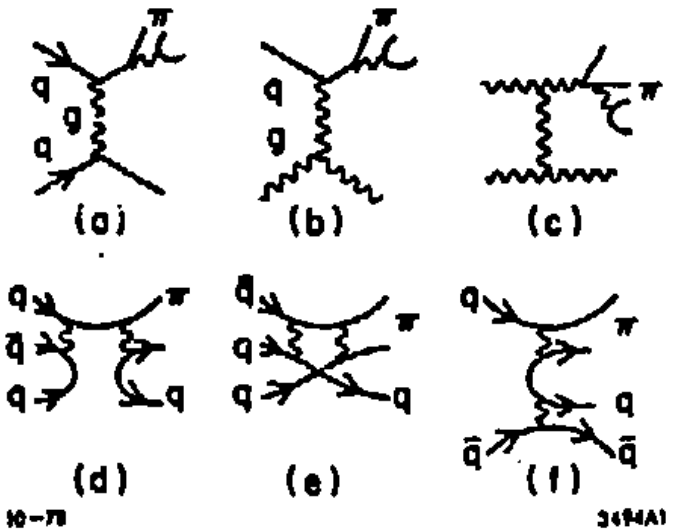


Fig. 1

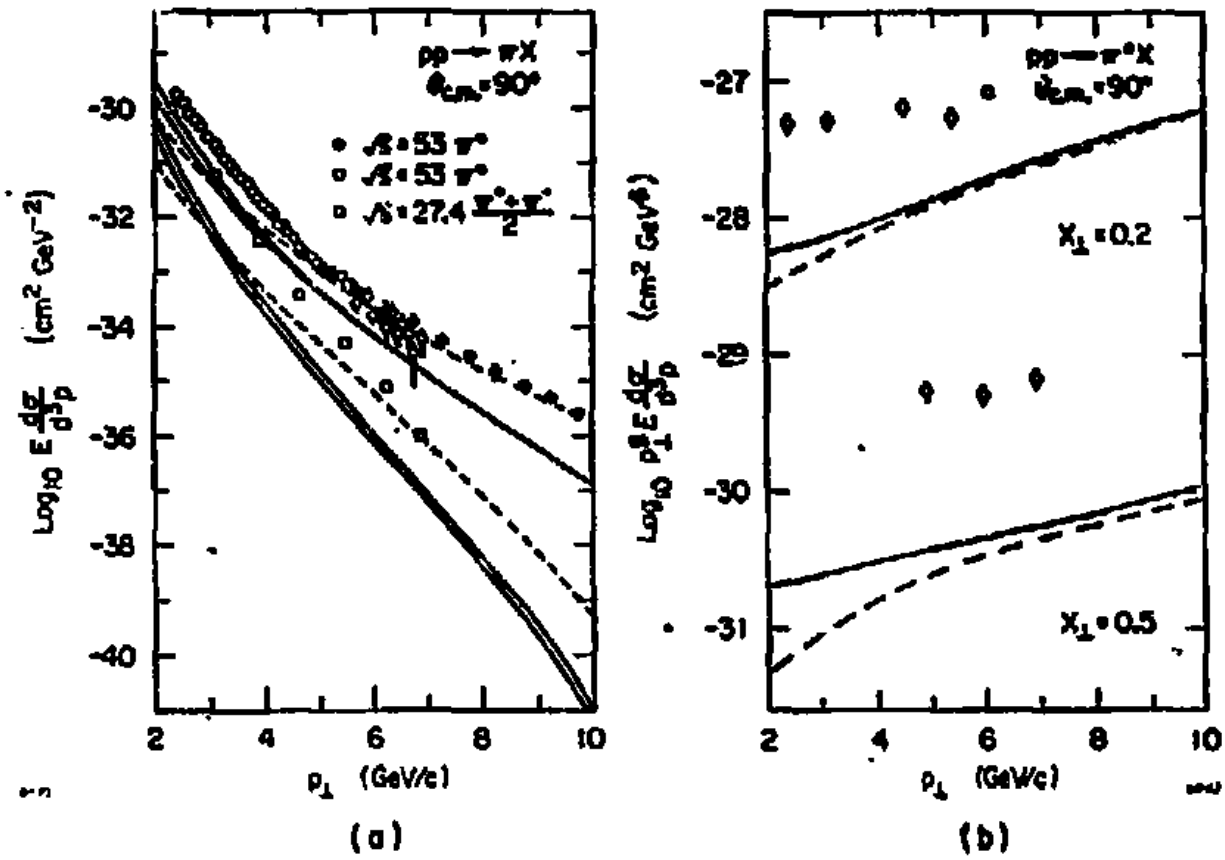
pp → π⁰X
θc.m.=90°
√s=53 π⁰
√s=53 π⁰
√s=27.4 π⁰+π⁻/2
Log10 E d³σ/dp³ (cm² GeV⁻²)
-30
-32
-34
-36
-38
-40
2
4
6
8
10
p⊥ (GeV/c)
(a)
pp → π⁰X
θc.m.=90°
X⊥=0.2
X⊥=0.5
Log10 p⊥⁴ E d³σ/dp³ (cm² GeV⁻²)
-27
-28
-30
-31
2
4
6
8
10
p⊥ (GeV/c)
(b)

Fig. 2

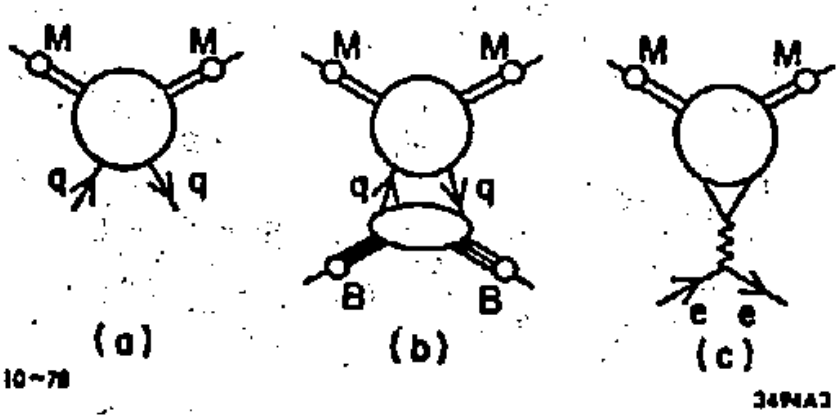


10-78

3494A3

Fig. 3

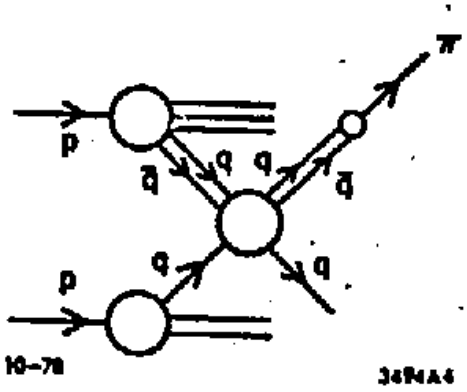


Fig. 4

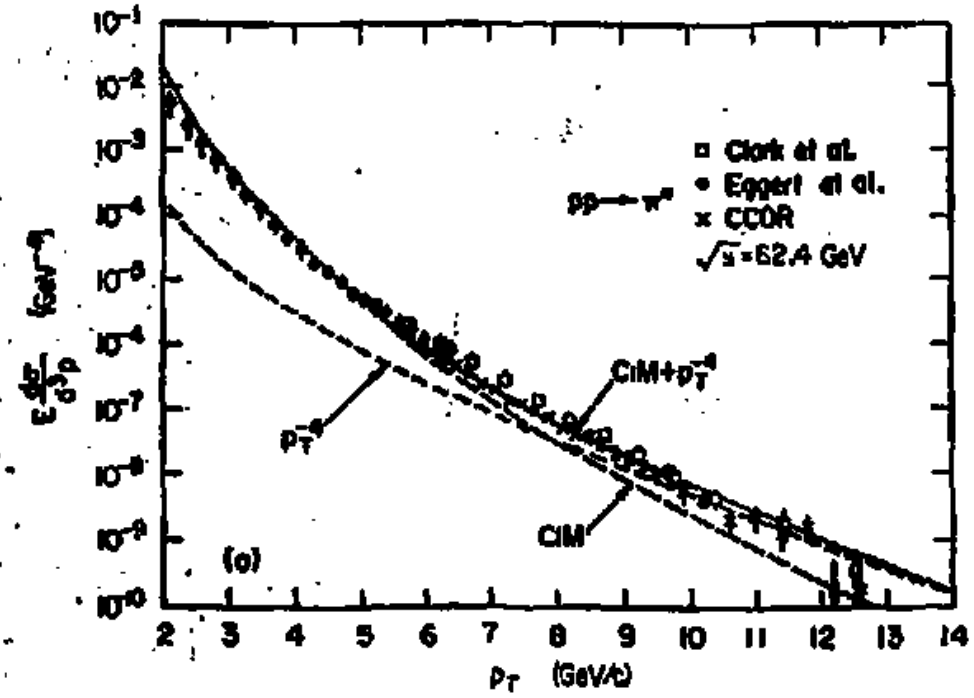
Clark et al.
Eggert et al.
CCOR
√s=62.4 GeV
pp→π⁰
CIM+p_T^-4
p_T^-4
CIM
(a)
p_T (GeV/c)

Fig. 5

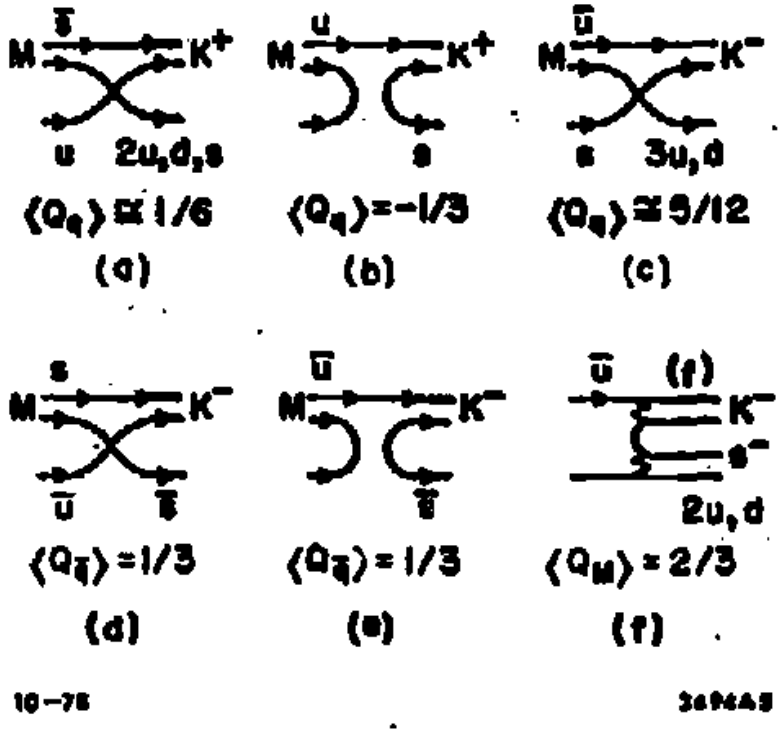
M
K+
u 2u,d,s
⟨Q_q⟩ ≅ 1/6
(a)
M
K+
s
⟨Q_q⟩=-1/3
(b)
M
K-
s 3u,d
⟨Q_q⟩ ≅ 5/12
(c)
M
K-
ū s̄
⟨Q_q̄⟩ = 1/3
(d)
M
K-
s̄
⟨Q_q̄⟩ = 1/3
(e)
(f)
K-
2u,d
⟨Q_M⟩ = 2/3
(f)
10-75
3494A8

Fig. 6

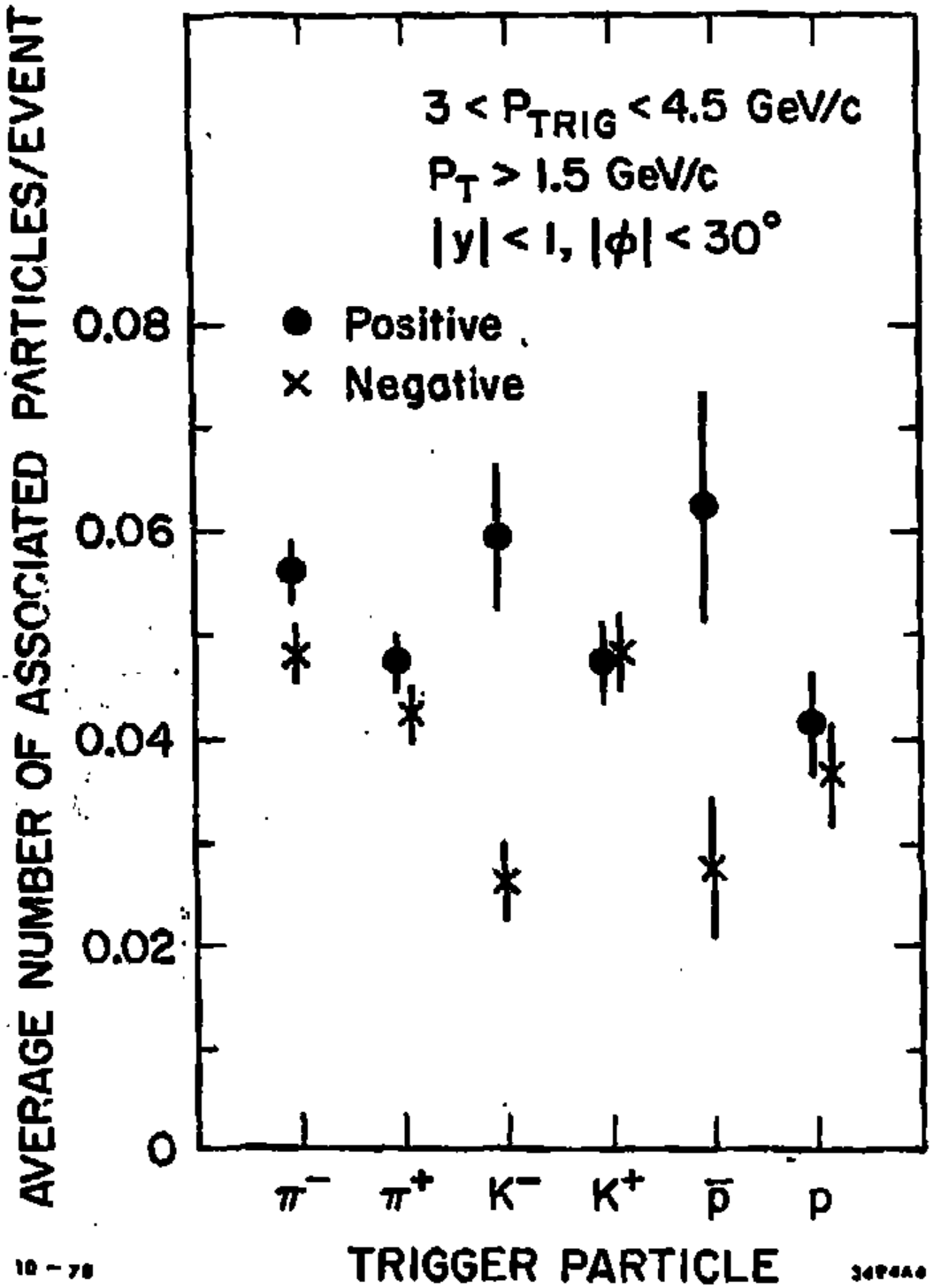
3 < P_TRIG < 4.5 GeV/c
P_T > 1.5 GeV/c
|y| < 1, |φ| < 30°
Positive
Negative
AVERAGE NUMBER OF ASSOCIATED PARTICLES/EVENT
0.08
0.06
0.04
0.02
0
π⁻ π⁺ K⁻ K⁺ p̄ p
TRIGGER PARTICLE

Fig. 7

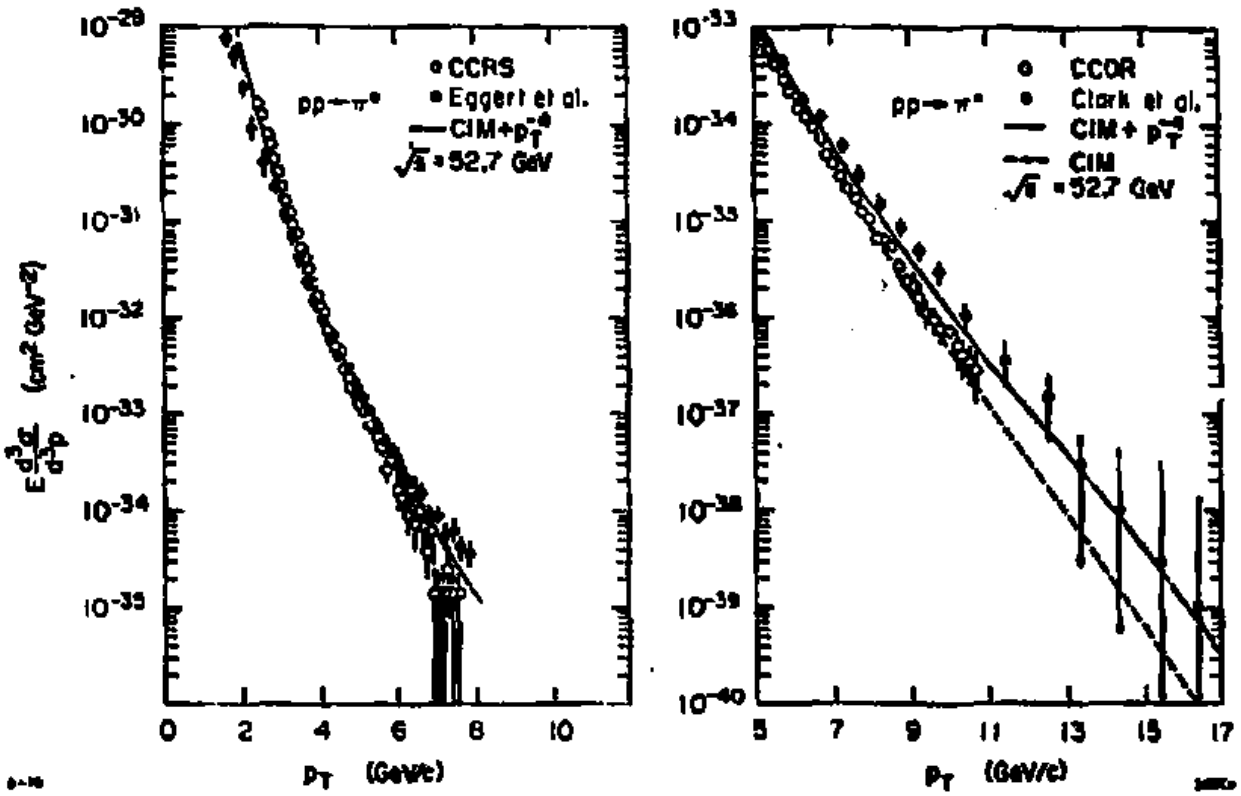
CCRS
Eggert et al.
CIM+$p_T^{-8}$
$\sqrt{s}$ = 52.7 GeV
$pp \to \pi^0$
$E\frac{d^3\sigma}{d^3p}$ (cm² GeV⁻²)
$p_T$ (GeV/c)
CCOR
Clark et al.
CIM + $p_T^{-8}$
CIM
$\sqrt{s}$ = 52.7 GeV
$pp \to \pi^0$
$p_T$ (GeV/c)

Fig. 8

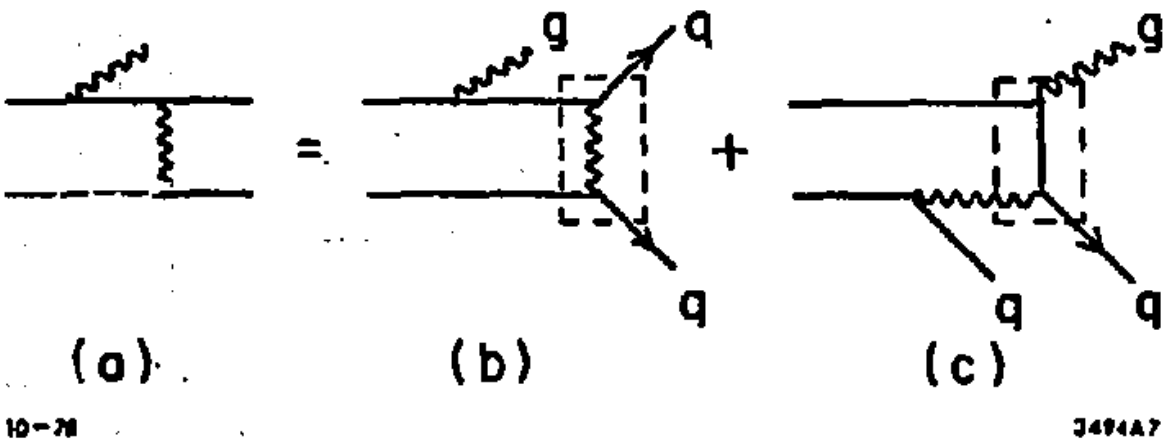


Fig. 9

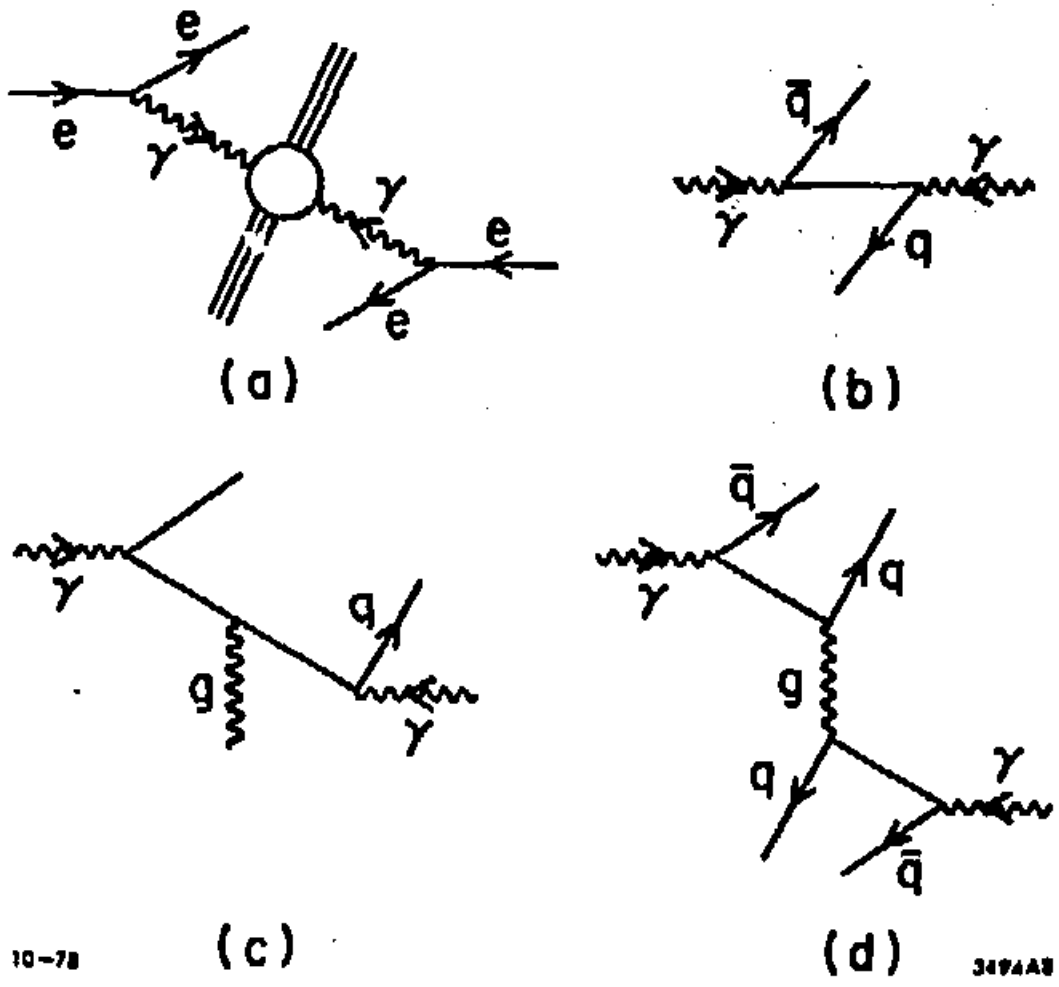


Fig. 10

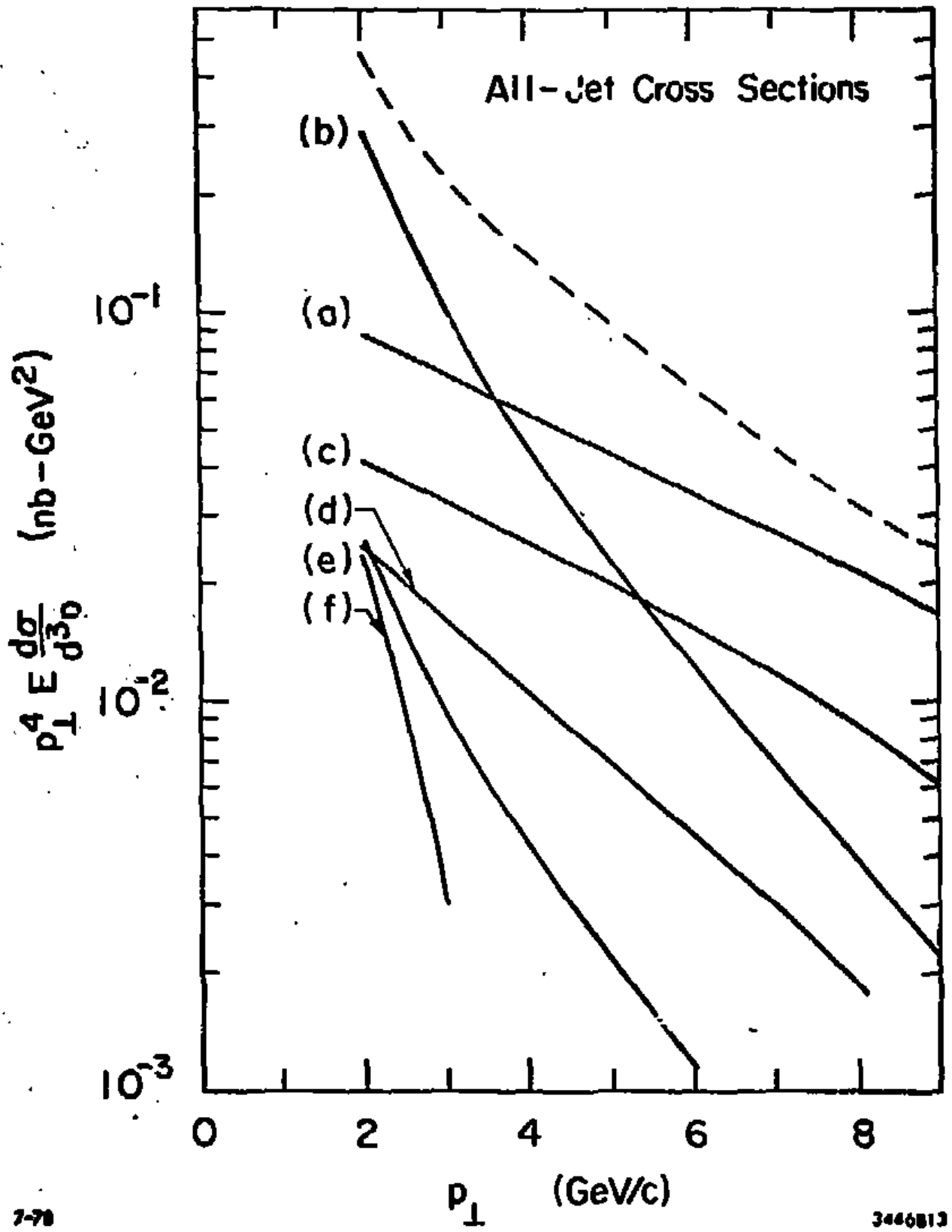
All-Jet Cross Sections
(b)
(a)
(c)
(d)
(e)
(f)
$10^{-1}$
$10^{-2}$
$10^{-3}$
$p_\perp^4 E \frac{d\sigma}{d^3p}$ (nb-GeV$^2$)
0
2
4
6
8
$p_\perp$ (GeV/c)
7-78
3446B13

Fig. 11

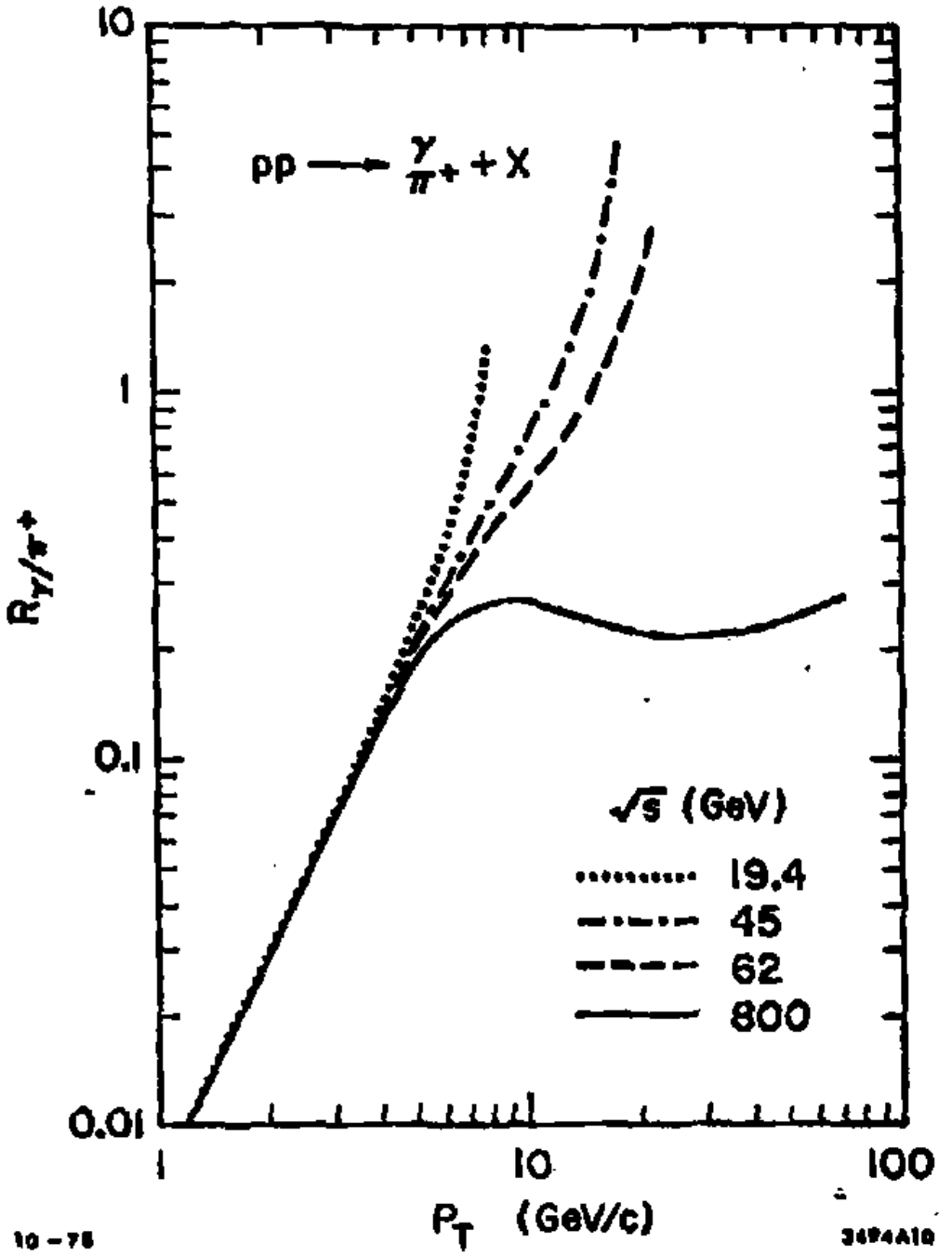
10
1
0.1
0.01
$pp \longrightarrow \frac{\gamma}{\pi^+} + X$
$R_{\gamma/\pi^+}$
$\sqrt{s}$ (GeV)
19.4
45
62
800
1
10
100
$P_T$ (GeV/c)
10-75
3694A10

Fig. 12

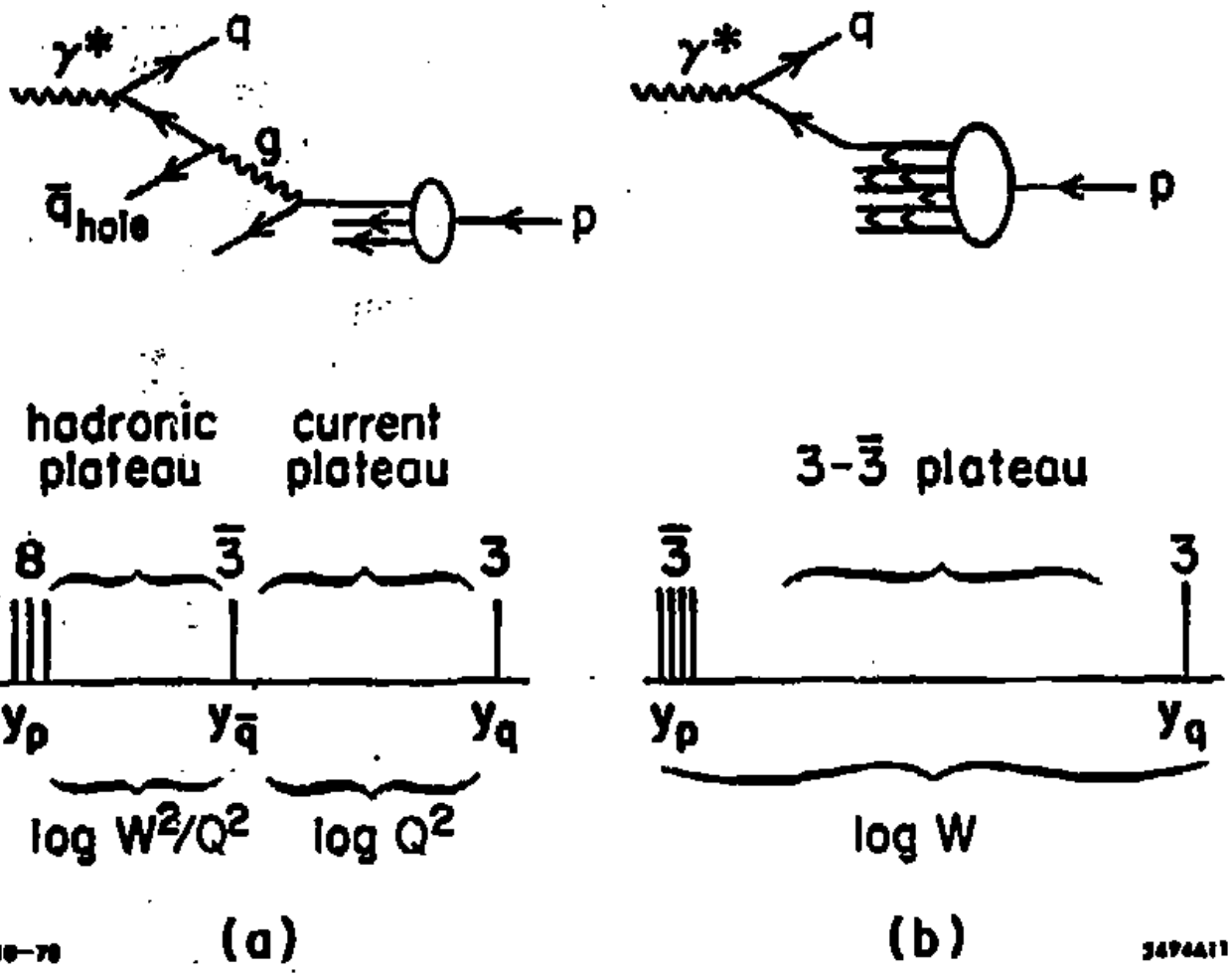
γ*
q
g
q̄hole
p
γ*
q
p
hadronic plateau
current plateau
8
3̄
3
yp
yq̄
yq
log W²/Q²
log Q²
(a)
3-3̄ plateau
3̄
3
yp
yq
log W
(b)

Fig. 13

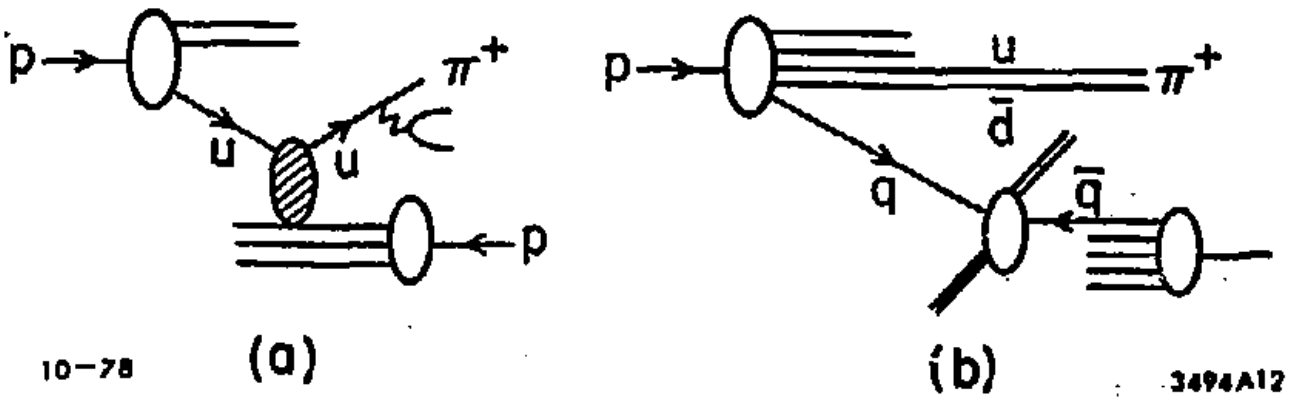


Fig. 14

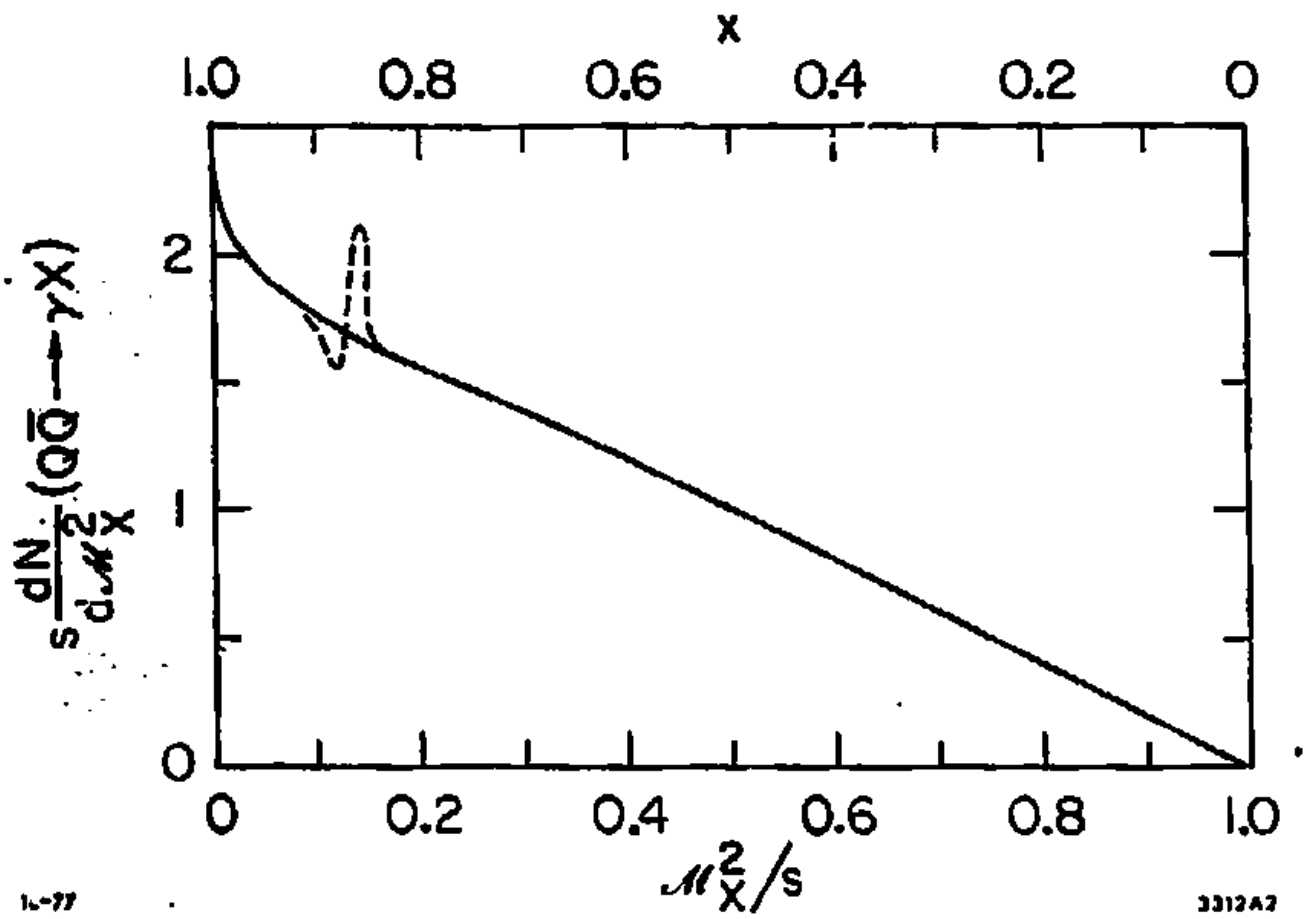
x
1.0
0.8
0.6
0.4
0.2
0
2
1
0
0
0.2
0.4
0.6
0.8
1.0
$s\frac{dN}{dM_X^2}(Q\bar{Q}\to\gamma X)$
$M_X^2/s$
3312A2

Fig. 15

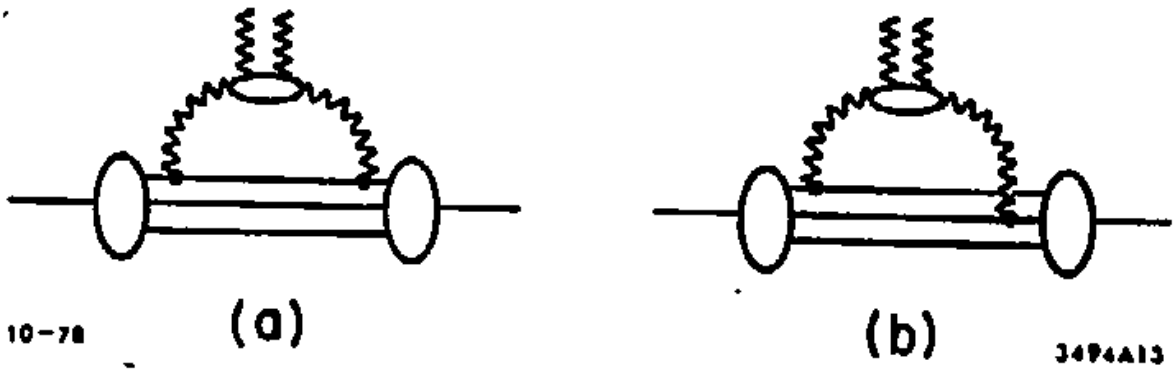


Fig. 16